Bulletin of Faculty of Science, Zagazig University (BFSZU)
e-ISSN: 1110-1555
Volume-2024, Issue-3, pp-197-224
https://bfszu.journals.ekb.eg/journal
Research Paper DOI: 10.21608/bfszu.2024.324408.1431

==

Petrophysical and Petrographical Studies for Abu Madi Reservoir in West Al Khilala Field, Nile Delta, Egypt: Insights for Optimized Hydrocarbon Production

Emad A. Eysa[1], A. A. El Khadragy[1], A. Abd El Kader[2], A. Hashim[3].

[1]Geology Department, Faculty of Science, Zagazig University, Egypt
[2]Mansoura Petroleum Company, Egypt
[3]Petroceltic Company, Egypt
***Corresponding author**: emad_eysa@zu.edu.eg

ABSTRACT **: The main objective of the present study aims to comprehensively evaluate the different properties of the Late Miocene Abu Madi Reservoir in West Al Khilala Field by analyzing petrophysical data from two wells. The goals of this study are summarized in the following points: characterizing the lithological composition and petrophysical properties of the reservoir intervals, Identifying hydrocarbon-bearing zones and assessing their potential for commercial production, evaluating the heterogeneity and continuity of the reservoirs to optimize well placement and completion designs, understanding the mineralogical composition and diagenetic processes influencing reservoir quality, and providing insights into the geological and petrophysical factors controlling reservoir behavior and performance.**

The petrophysical evaluation of Abu Madi Reservoir in W. Al Khilala-2 and W. Al Khilala-5 wells in the study area reveals distinctive reservoir characteristics. In W. Al Khilala-2, a sandstone interval with hydrocarbon shows was identified between depths of 9920 to 10090 FT.MD. It features a gross reservoir thickness of 170 FT and a net thickness of 114.5 FT. Effective porosity ranged from 15.4% to 26%, with a shale content of approximately 14%. This consistent lithological homogeneity suggests favorable reservoir quality.

Conversely, W. Al Khilala-5 exhibits a hydrocarbon-bearing interval within the Abu Madi Reservoir, showcasing 58.5 FT of gross sandstone thickness between depths of 10221.5 and 10280 FT.MD. The net pay thickness is 23 FT., with an average effective porosity of 19.4% and water saturation ranging from 39.1% to 73.5%. Notably, resistivity readings exhibit significant variation, forming a funnel shape, while the shale content remains relatively low at about 11.3%.

Additionally, core data analysis corroborates these findings. For W. Al Khilala-2, the reservoir displays heterogeneity characterized by subfeldspathic arenite with variable hydrocarbon and water saturation levels. In W. Al Khilala-5, sandstone predominance is observed, albeit with decreased porosity due to the presence of siltstones and poorly sorted sandstone facies. The reservoir characterized by very good porosity and permeability. The porosity was homogenous where the permeability was heterogeneous.

Petrographic analysis reveals significant detrital components such as quartz, feldspar, glauconite, lithic fragments, micas, and heavy minerals, influencing reservoir composition and behavior. Authigenic components like calcite, quartz overgrowths, kaolinite, siderite, chlorite, and illite contribute to pore space alteration and porosity reduction, influencing permeability in both wells.

Overall, the reservoirs exhibit varying lithological characteristics and petrophysical properties, highlighting the need for comprehensive analysis to understand their behavior and optimize production strategies.

KEYWORDS: West Al Khilala, Abu Madi, Petrophysical Characterization, Petrography and Nile Delta.

Date of Submission: 28-09-2024 Date of acceptance: 16-10-2024

I. INTRODUCTION

Recently, many oil and gas companies had discovered several gas and oil fields in the Nile Delta. Therefore, geophysical and geological studies, especially seismic data, petrophysical evaluation and modeling are important. They play the main role in delineating reservoir boundaries and petrophysical parameters. The petrophysical evaluation of reservoirs plays a pivotal role in the exploration and production of hydrocarbon resources.

Understanding the characteristics and behavior of subsurface formations is crucial for optimizing drilling strategies, estimating reserves, and maximizing production efficiency. In this paper, we focus on the assessment of Abu Madi Reservoir in W. AL Khilala Field, utilizing data from two key wells, W. Al Khilala-2 and W. Al Khilala-5.

The investigated area in this study is a sector model of West Al Khilala gas field that located in the central onshore part of the Nile Delta (**Fig. 1**).

The hydrocarbon exploration In the Nile Delta region began in 1947 by the Standard Oil Company of Egypt (SOC), but the actual effective exploration activities did not started until 1963 (**EGPC, 1994**).

W. Al Khilala-1 Well was drilled in 2005 as an exploratory well. It penetrated the Abu Madi Formation to the depth of 11,250 FT.MD. Hydrocarbon significant gas shows recorded within the sandstones of Abu Madi Formation reached up to 101,000 PPM with components up to C3. The well was tested to produce gas and condensate with a gas rate of about 20.9 MMSCFPD on a choke size of 32/64" (**Mansoura Pet. Co., 2005**).

In April 2007, the W. Al Khilala-5 Well was drilled as a development well to increase the productivity of the hydrocarbons from the area, in addition to confirm the gas/water contact. Hydrocarbon significant gas shows were recorded up to 54,100 PPM within the Abu Madi sandstones with components up to NC4. The well tested as a gas producer with rate about 12.5 MMSCFPD on a choke size of 24/64" (**Mansoura Pet. Co., 2008d**).

2. Geologic Setting

The Nile Delta region in Egypt was subjected to intense geological and geophysical studies concerning finding gas and oil prospects. The subsurface and structural geology of the Nile Delta had been studied by eminent authors as **Schlumberger (1984); Said (1990); EGPC (1994); Harwood et al. (1998); Nashaat (1998 and 2000); Elgamal (2001 and 2002); El-Shafei (2004): Elbosraty (2005); Mahsoub (2006); Elgamal and Elbosraty (2008); Khaled et al. (2014); Elhamy and Salah (2016); Ismael et al. (2024)** and others.

The Nile Delta region occupies a key position within the plate tectonic framework of the eastern Mediterranean Sea and Levant Basin. It lies on the northern margin of the African plate, which extends from the subduction zone adjacent to the Crete and Cyprus arcs to the Red Sea, where it rifted a part of the Arabian plate (**EGPC, 1994**). It is subdivided into two areas with different tectonic characters. The northern offshore delta region is characterized by subsidence with thick Tertiary sedimentary pile, while the souther onshore delta region is characterized by shallower basement and commonly faulted blocks. The boundary between these regions is separated by a faulted flexure zone called hinge zone that layies at about latitude 31° N (**EGPC, 1994**).

According to **Abdel Aal et al. (1994)** and **EGPC (1994)**, the tectonic history of the Nile Delta region is subdivided into three main tectonic phases.

The First Tectonic Phase extendeds from Late Paleozoic to Early Mesozoic throughout E-W fault zone named the hinge zone (**Fig. 2**). Deep structures in the Nile Delta show that the hinge zone bisects the Nile Delta parallel to the pre-existing E-W fault trends.

From Triassic to Jurassic time, left lateral oblique-slip extension in northern Egypt occurred, which was associated with the opening of the Tethys Sea as the result of the movement of Eurasia away from Africa (**Argyriadis et al., 1980**) that is related to the development of the Miocene to recent Gulf of Aqaba rift. The main expressions of this movement are NE-SW to ENE-SSW trending normal fault.

The Second Tectonic Phase began from Late Cretaceous to Early Tertiary, where Egypt was affected by NW-SE oblique compression force. This oblique compression produced a series of NW-SE trending doubly plunging anticlines (Syrian Arc structures) in the northern Sinai and in the Western Desert. This force produced a series of the NW-NNW extension faults parallel to the major compression stresses that affected northern Egypt (**Fig. 2**).

The Third Tectonic Phase extended from Late Eocene to Recent, which is dominated by three main structural trends. NNW normal trending faults, which are present in the central part of the Nile Delta and parallel to the Gulf of Suez rift that extended from Late Eocene to Miocene Gulf of Suez trend. NNE normal trending faults, which are observed parallel to the Rosetta fault trend and related to the development of the Miocene to Recent Gulf of Aqaba rift. NS Baltim structural fault trend that is mapped in particular at the western side of the Qatarra depression, which was formed by rejuvenation and reactivation of the older Pre-Tertiary structures during the Early Miocene.

The stratigraphic and sedimentological frameworks of the Nile Delta are subdivided into western, central, eastern and offshore regions. These regions showed great variation In facies and thickness. These variations can be explained to a large extent in terms of tectonic events (**El Heiny, 1982; El Heiny and Morsi, 1992**). The stratigraphic sequence in the Nile Delta province is represented by Jurassic to Pleistocene facies (**Fig. 3**).

The hydrocarbon potentiality of the Nile Delta sedimentary sequence is limited for the time being to the Neogene formations, trapped against listric fault planes or over tilted faulted blocks. However, Pre-Miocene formations, which form the base of the Neogene sequence may also be taken into consideration as having hydrocarbon potentialities. They are confirmed to the platform and its edge along the hinge zone where they could be developed as high energy deposits such as reefal build-ups. North of the hinge zone they may be adversely affected by the normal down-to basin, step faulting (**EGPC, 1994**).

Fig. 1: Location map of West Al Khilala Field (Study Area).

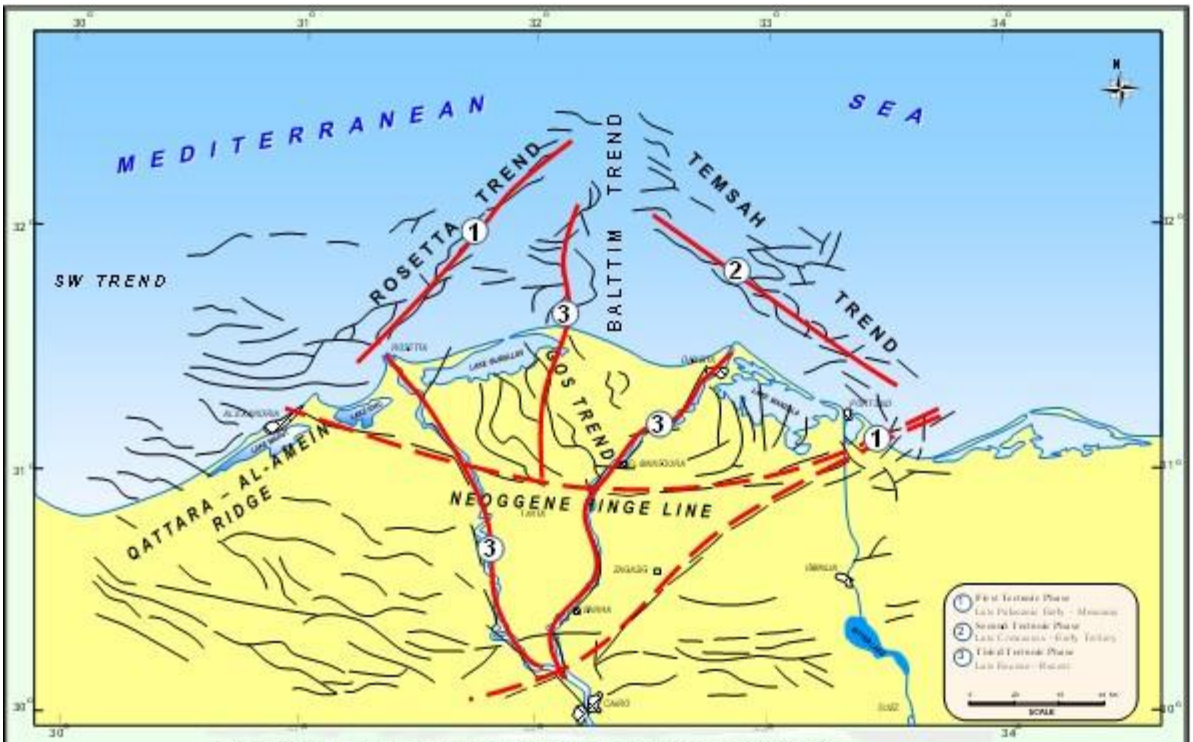

Fig.2: Nile Delta tectonic setting map, (Abd El Al *et al*, 1994)

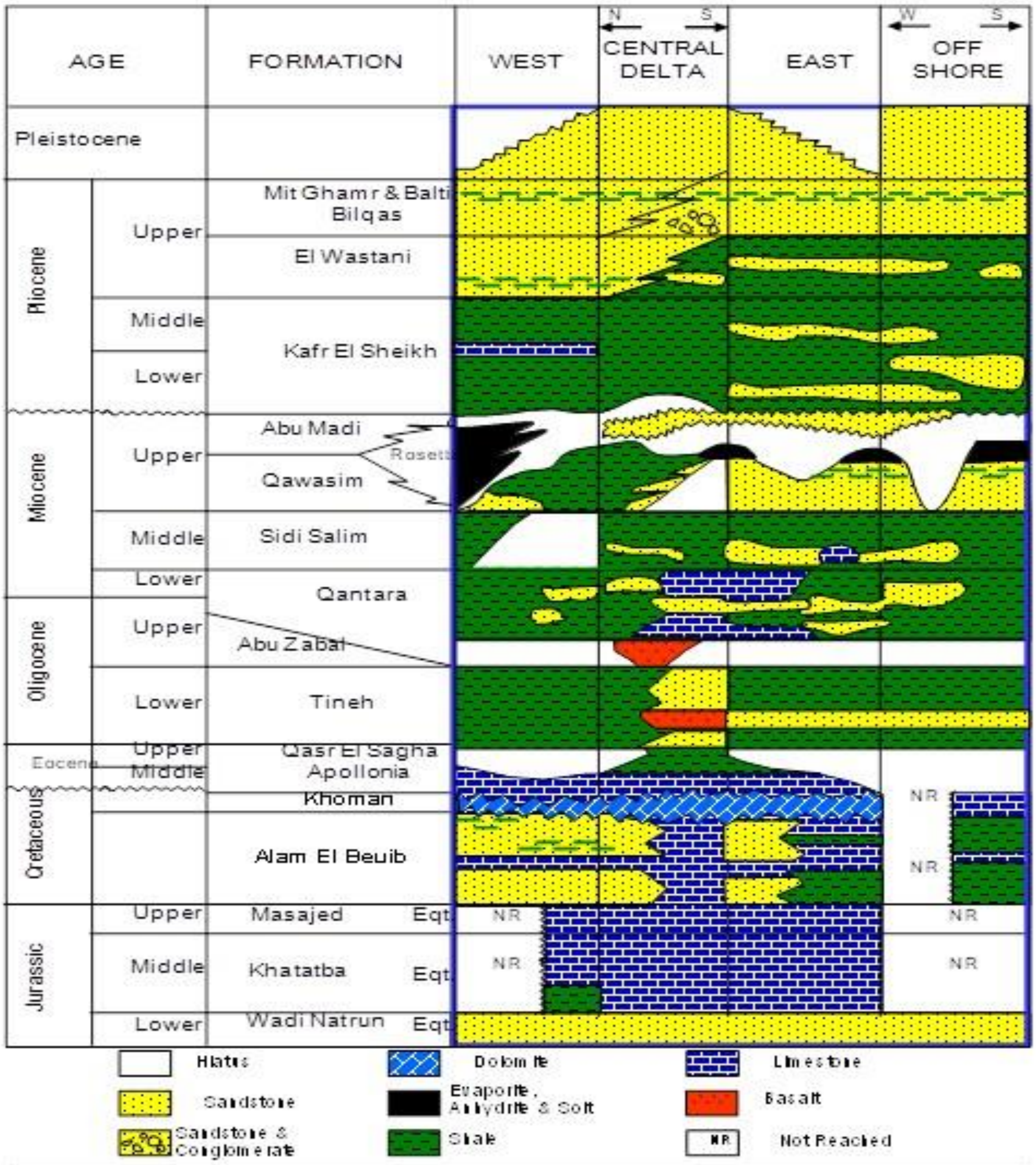

Fig. 3: Generalized lithostratigraphic sections of the Nile Delta (EGPC, 1994).

The Miocene deposits start with open marine sediments and ends with a great evaporitic sequence. It can be divided into Qantara, Sidi Salim, Qawasim, Abu Madi and Rosetta formations, from base to top respectively.

Abu Madi Formation is composed of thick conglomeritic sand layers, interbedded with shale layers, which increase in thickness in the upper part of the formation. The sand is quartzose, variable in grain size and almost loose. The conglomerates levels in the lower part of the formation exhibit an unconformity having a sandy matrix.

EGPC (1994); El Heiny and Enani (1996) defined the sedimentary structure of Abu Madi Formation as cross-bedded sandstone and the shale content is increasing upwards. **Rizzini et al. (1978)** indicated that this formation has deltaic origin and grades up into a shallow marine environment. Abu Madi Formation is the main gas-producing horizon in the Nile Delta containing the sandstone, which can be considered to be the best reservoirs in the Nile Delta, as they have a high porosity with an average about 21% (**EGPC, 1994**).

3. Material and methods

The present study aims to investigate the different properties of the Late Miocene Abu Madi Reservoir in West Al Khilala Field throughout application of different steps. The first step is to determine the different petrophysical parameters that characterize the concerned reservoirs. The second is to characterize the different facies within the reservoir sediments. The third is to determine the lithological component of the reservoir using the conventional core data analysis.

The available materials for the present study were provided by Egyptian General Petroleum Corporation (EGPC) throughout Petroceltic Petroleum Company. It includes Electric logging data and conventional core data reports for two wells. Interactive Petrophysical Computer Software (IP. V. 4.0) and Microsoft office (Excel 2013) were used in petrophysical evaluation.

4. Results and discussion

4.1 Petrophysical evaluation

Two main wells (W. Al Khilala-2 & 5) were used to evaluate the reservoir characterization in the W. AL Khilala Field using the Interactive Petrophysics software (IP). The Abu Madi Formation in W. Al Khilala-2 well characterized by a thick shale body with a sandstone interval having hydrocarbon shows (**Fig. 4**). Throughout the formation evaluation, the sandstone interval was deduced at the interval of 9920 FT.MD. to 10,090 FT.MD. with gross thickness of 170 FT and net thickness of 114.5 FT. The sandstone characterized by effective porosity ranged from 15.4% to 26% with an average of 20.6%. The average shale content was about 14%, which reflects the lithological homogeneity.

In W. Al Khilala-5 Well, the hydrocarbon bearing interval in the Abu Madi Formation is medium to coarse grained and moderately sorted sandstone. It characterized by calcareous and argillaceous cement with glauconitic and pyritic fragments (**Mansoura Pet. Co., 2008d**).

The petrophysical results (**Fig. 5**) illustrate a thick shale body in the hydrocarbon bearing sandstone main interval. The gross sandstone thickness is about 58.5FT. (from 10,221.5 FT.MD. to 10,280 FT.MD. depth). The net pay thickness is 23FT. It is characterized by average effective porosity of 19.4% and average water saturation about 57.7%. It also reflects a high change in resistivity reading values throughout the reservoir appearing in a funnel shape. The average shale content is about 11.3% reflects the lithological homogeneity for the reservoir interval.

4.2 Statistical analysis and histograms of core DATA.

Core analysis is a tool in reservoir assessment that directly measures many important formation properties. The analysis may aim to determine porosity, permeability, fluid saturation, grain size distribution, mineral composition, grain density, etc. Samples for this analysis may come from the conventional core, sidewall cores or plugs, and cuttings (**Bateman, 1985**). The samples of the cores cleaned and dried prior to testing (restored core). This analysis was performed in two wells W. Al Khilala-2 and 5 by core laboratory in order to determine the petrophysical properties of Abu Madi Reservoir.

In the most reservoir types the porosity ranges from 5% to 30% and the porosity of reservoir can be classified, according to **Levorson (1967)**, into five categories as Negligible (0-5%), Poor (5-10%), Fair (10-15%), good (15-20 %) and very good porosity (20-25 %).

The conventional core is prepared by Corex Services LTD for **Mansoura Petroleum Company (2006)**. The porosity analysis in the present study is completed using helium porosity.

Table (1) illustrates the summary of descriptive statistical analysis for the porosity data of the analyzed samples. There were 127 samples from W. Al Khilala-2 and 56 sample from W. Al Khilala-5in the studied wells, which calculated using the Microsoft Excel 2013 program.

The analysis of W. Al Khilala-2 Well display that the porosity values ranges from 4.6 % to 33.22 % with mean value 27.79%. Where in W. Al Khilala-5 Well the values ranged from 8.10 % to 31 % with a mean value 24.96%. The stander deviation values are 3.16 and 3.65 indicating homogeneous reservoir with good characteristics

The helium porosity histogram and cumulative frequency for the studied samples in W. Al Khilala-2 and 5 wells are represented in **figures (6 & 7)**. About 98% of W. Al Khilala-2 samples have porosity values larger than porosity 20%. While in W. Al Khilala-5 about 94% of the studied samples have porosity values larger than the porosity 20%. The previous results indicated that the Abu Madi Reservoir in W. Al Khilala-2 and 5 wells have very good porosity.

Permeability of petroleum reservoir rocks may ranges from 0.1 to 1000 or more millidarcies. **Leverson, 1967** classified the quality of a reservoir based on permeability into fair ($1 < k < 10$), good ($10 < k < 100$), Very good ($100 < k < 1000$) and Excellent ($k > 1000$ mD).

Table (2) illustrates the summary of descriptive statistical analysis of the horizontal and vertical permeability of the analyzed samples.

About 123 samples from W. Al Khilala-2 and 52 samples from W. Al Khilala-5 were used to study the horizontal and vertical permeability of Abu Madi Reservoir. The horizontal permeability values in W. Al Khilala-2 Well varies from 1.1 mD to 1953 mD with a mean value of 421 mD and stander deviation 374. The horizontal permeability in W. Al Khilala-5 ranged from 3.39 mD to 1129 mD with mean value of 305 mD and stander deviation of 266.

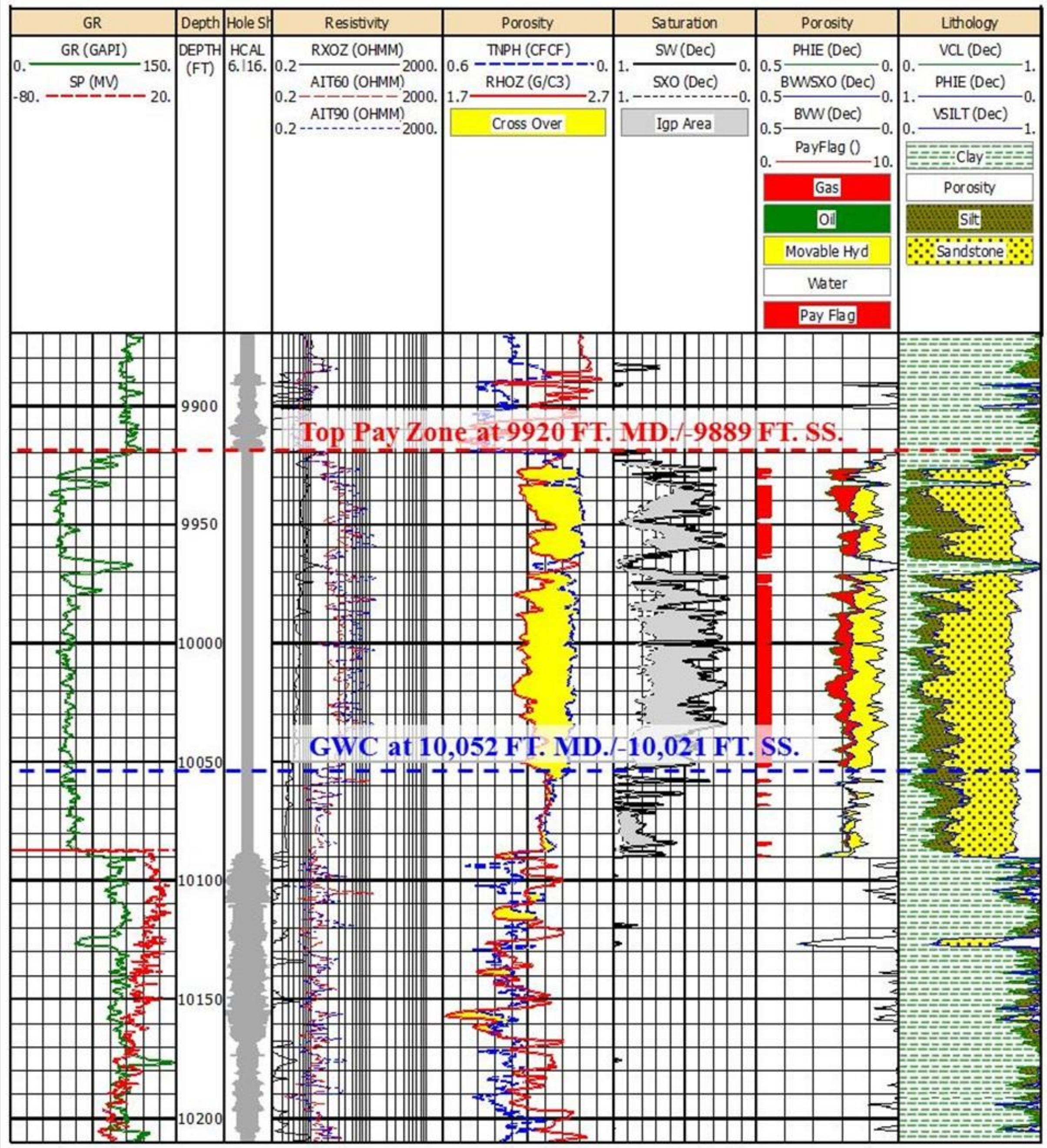

Fig. 4 : Litho-saturation crossplot of the Late Miocene Abu Madi Fm., W. Al Khilala-2 Well.

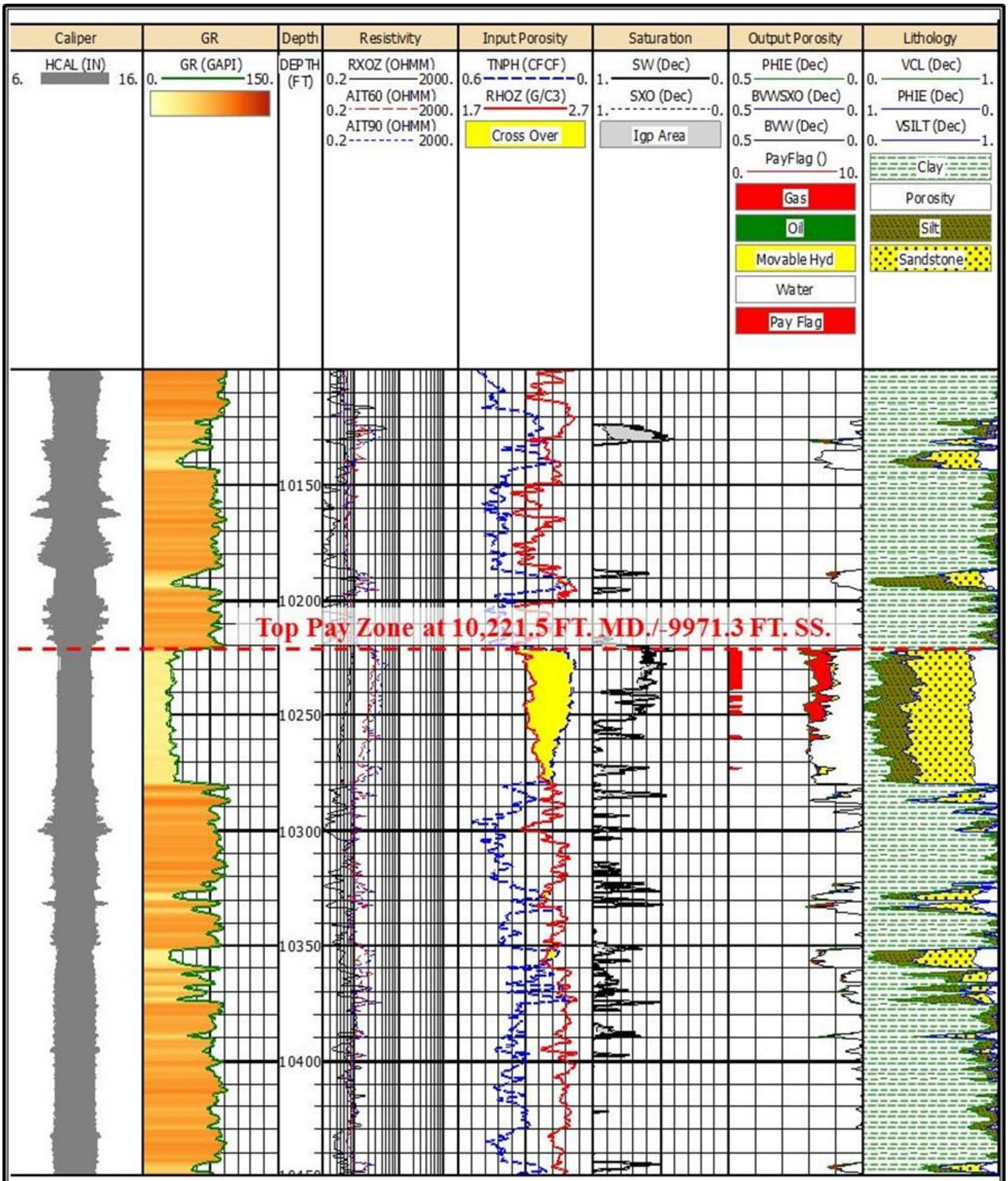

Fig. 5 : Litho-saturation crossplot of the Late Miocene Abu Madi Fm., W. Al Khilala-5 Well.

Table (1): Descriptive statistical analysis for porosity of Abu Madi Reservoir in W. Al Khilala-2 and 5 wells.

	W. Al Khilala-2	W. Al Khilala-5
Descriptive Statistics	**Helium porosity (ϕ_h), %**	**Helium porosity (ϕ_h), %**
Mean	27.79	24.96
Median	28.28	25.10
Mode	N/A	25.10
Standard Deviation	3.16	3.65
Minimum	4.60	8.10
Maximum	33.22	31
Sum	3529.58	1397.8
Count	127	56

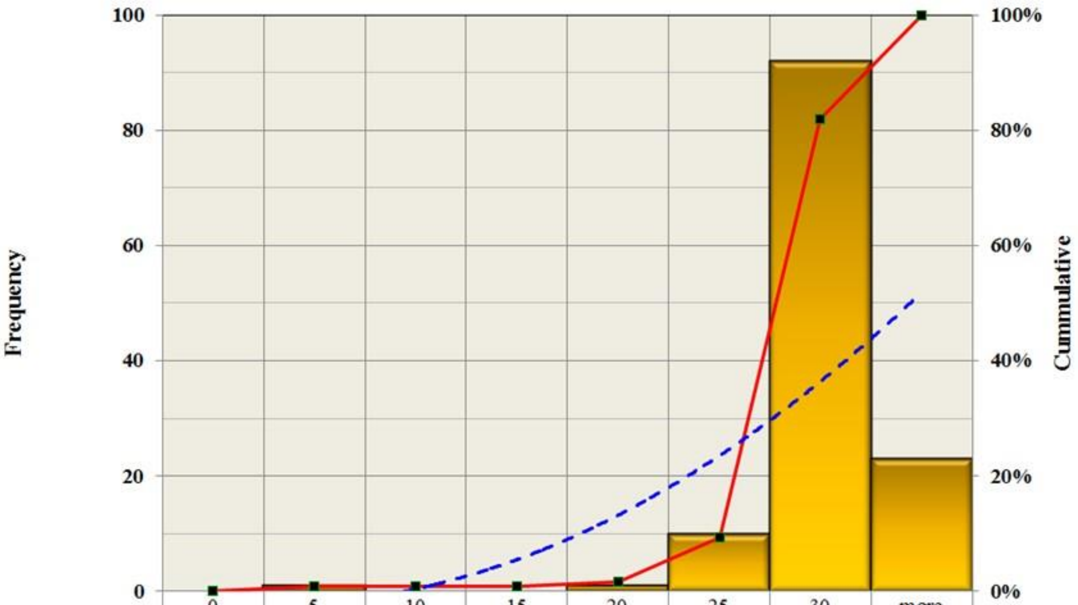

	0	5	10	15	20	25	30	more
Frequency	0	1	0	0	1	10	92	23
Cummulative	0%	1%	1%	1%	2%	9%	82%	100%

Helium Porosity

Fig. 6: Histogram and cumulative frequency of helium porosity for Abu Madi Reservoir in W. Al Khilala-2 Well.

	0	5	10	15	20	25	30	More
Frequency	0	0	1	1	0	24	29	1
Cumulative %	0%	0%	2%	4%	4%	46%	98%	100%

Fig. 7: Histogram and cumulative frequency of helium porosity for Abu Madi Reservoir in W. Al Khilala-5 Well.

Table (2): Descriptive statistical analysis of the horizontal and vertical permeability for Abu Madi Reservoir in W. Al Khilala-2 and 5 wells.

Descriptive Statistics	W. Al Khilala-2		W. Al Khilala-5	
	Horizotal permeability (Kh) md.	Vertical permeability (Kv) md.	Horizotal permeability (Kh) md.	Vertical permeability (Kv) md.
Mean	421	340	305	214
Median	308	272	263	191
Mode	310	417	275	144
Standard Deviation	374	317	266	166
Minimum	1.1	2.7	3.39	1
Maximum	1953	1775	1129	758
Sum	51783	41827	15842	11139
Count	123	123	52	52

The vertical permeability in W. Al Khilala-2 Well ranged from 2.7 mD to 1775 mD with a mean value 340 mD and stander deviation of 317. In W. Al Khilala-5 Well, it ranged from 1 mD to 758 mD, with a mean value of 214 mD and stander deviation of 166. These values indicate very good heterogeneous permeability.

The histogram and cumulative frequency of horizontal permeability in W. Al Khilala-2 Well is showed in (**Fig. 8**). About 86% of the studied samples have a horizontal permeability values larger than 100 mD. In W. Al Khilala-5 Well, about 77% of the samples have a horizontal permeability larger than 100 mD (**Fig. 9**).

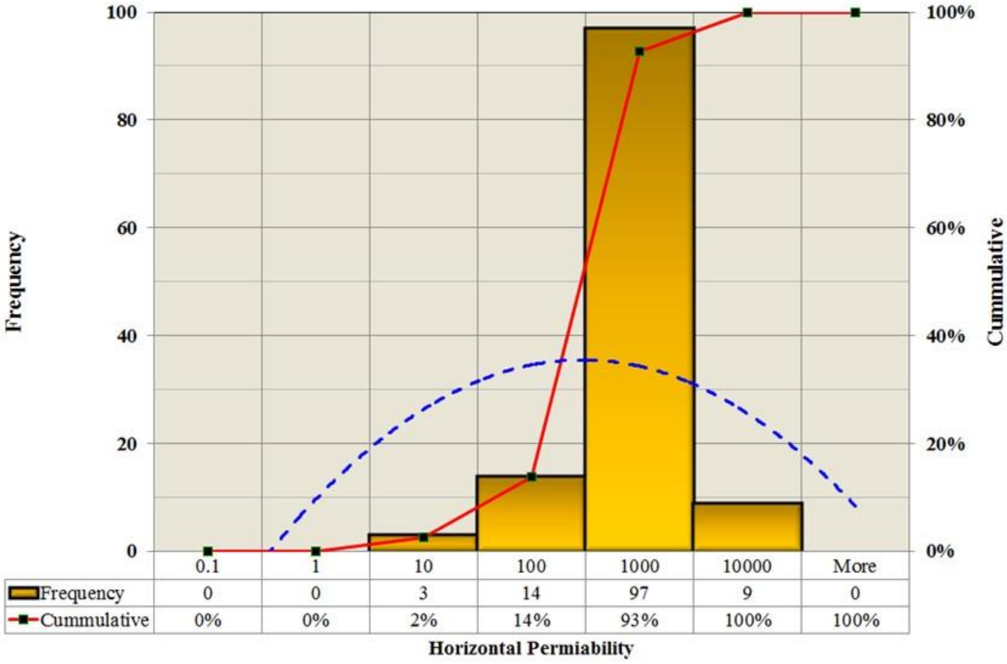

Fig. 8 : Histogram and cumulative frequency of horizontal permeability for Abu Madi Reservoir in W. Al Khilala-2 Well.

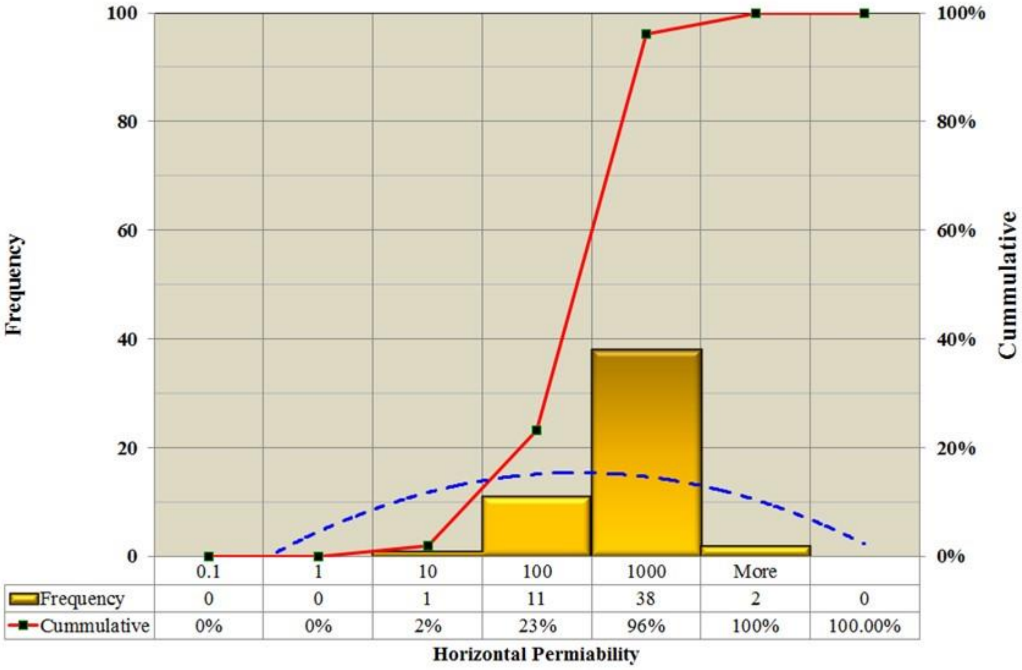

Fig. 9 : Histogram and cumulative frequency of horizontal permeability for Abu Madi Reservoir in W. Al Khilala-5 Well.

Figure (10) represented the vertical permeability histogram in W. Al Khilala-2 Well. It display that there are about 86 % of the samples have permeability values largre than 100 mD. On the other hand, about 71% of the samples have values larger than 100 mD in W. Al Khilala-5 (**Fig. 11**). The analysis indicated that the Abu Madi reservoir in W. Al Khilala-2 and W. Al Khilala-5 wells have very good to excellent horizontal and vertical permeability which aid in the process of hydrocarbon production.

This means that the vertical permeability in the Abu Madi Reservoir in W. Al Khilala-5 Well ranges from very good to excellent.

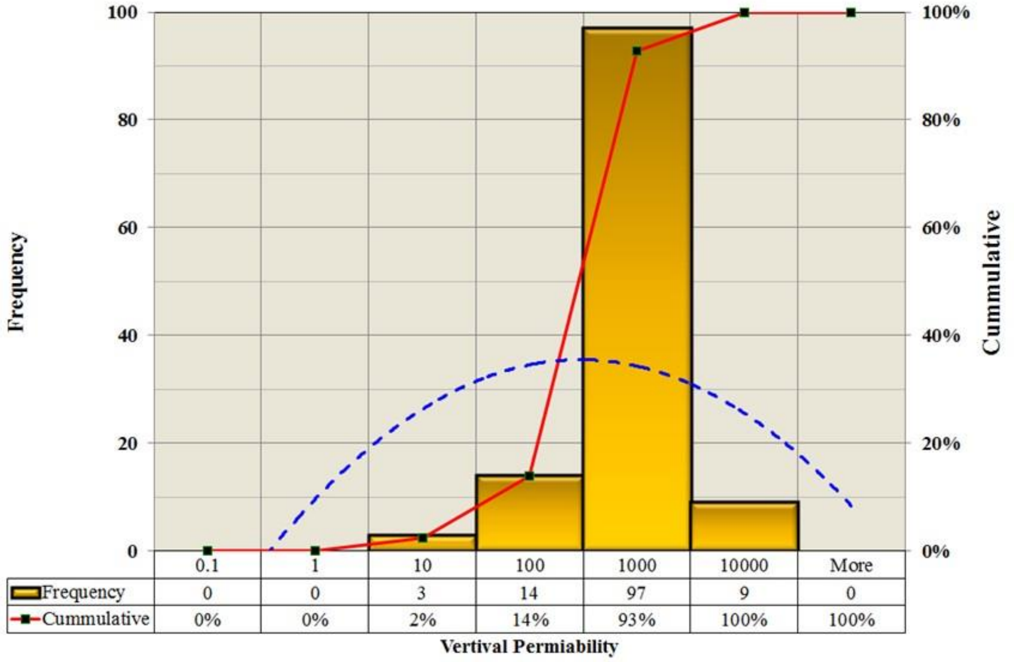

Fig. 10: Histogram and cumulative frequency of vertical permeability forAbu Madi Reservoir in W. Al Khilala-2 Well.

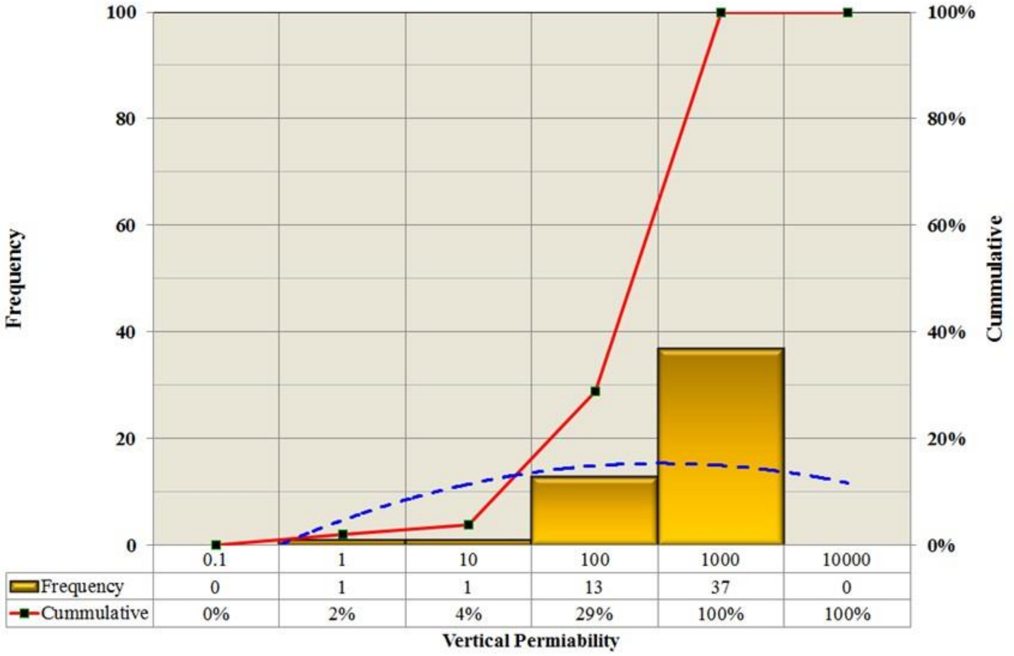

Fig. 11: Histogram and cumulative frequency of vertical permeability for Abu Madi Reservoir in W. Al Khilala-5 Well.

4.3 Core Data Evaluation

The Core Data for W. Al Khilala-2 Well revealed reservoir Heterogenity for the Abu Madi pay zone. The rock type was subfeldspathic arenite. It is characterized by fine to medium grain size, occasionally coarse to very coarse size, moderately to well sorted, highly to patchy cemented and poorly compacted with points and long and concave-convex grain contact. The hydrocarbon saturation is about 61.2% and the water saturation is about 38.8% which is not constant throughout the reservoir due to the resistivity effect (**Fig. 12**).

In W. Al Khilala-5 Well, the reservoir is characterized by the abundance of sandstone, which reveals the predominance of siltstones that tend to decrease the porosity throughout the reservoir interval. Several thin section samples in the reservoir display poorly sorted sandstone facies intervals (**Fig. 13**). It is composed of very fine to medium grains of sandstone that have a reverse effect on the effective porosity of the reservoir. The grains are well-cemented and moderately compacted with points and concave-convex grain contact. Minor dispersed pore filling and grain coating detrital clay matrix are common in the reservoir that also decrease the effective porosity.

4.4 Reservoir Rock Composition

Descriptions of rock fabric and texture have great value to petrophysicists. They can be used in facies analysis and in the interpretation of the depositional environment.

The petrographic point counting was used to determine the mineralogy of the sandstone reservoir in the Abu Madi Formation. The average minerals were analyzed based on 200 counts per slide. The mineral types recognized were quartz, feldspar, glauconite, lithic fragment, mica, heavy minerals and opaques, carbonaceous debris, phosphatic fragments, detrital clays and authoginic minerals. These composition results were illustrated in summary charts (**Fig. 14 & 15**).

4.4.1 Detrital Components

The detrital components of the rock form the major component of the reservoir, including the quartz grains, feldspar, glauconite, lithic fragment, mica, clay matrix, heavy minerals and opaques, carbonaceous debris, phosphatic fragments and detrital clays. They can be discussed in more detail in the following.

I. Quartz

The quartz grains are the most common detrital grain type in all examined samples in the reservoir interval. They typically from aout 10.5% to 69.5% of the sample volume in W. Al Khilala-2 Well (**Fig. 14**). They occur with relative abundances between 3.5% and 60% in W. Al Khilala-5 Well (**Fig. 15**). The grains ranged from fine to very coarse. In some coarse-grained sandstones, quartz grains can reach granule size. Most samples are composed of multi-celled quartz varieties, including dominantly inequigranular and equigranular types with long, pointer and concavo-convex contact boundaries (**Fig. 16**)

II. Feldspars

The feldspar is the second most abundant constituent. Its content ranges from traces to 7.5% with an average of 4.06% in W. Al Khilala-2 Well (**Fig. 14**), while in W. Al Khilala-5 Well it occurs with relative abundances between trace quantities and 3% by volume, whereas K-feldspars abundance was between trace quantities and 5% by volume (from depth 10336'03"FT.) (**Fig. 15**).

The plagioclase feldspars are common in all samples, where they occur with relative abundances ranging between trace quantities and 3% to 6% by volume for W. Al Khilala-2 & 5 Wells respectively (**Fig. 17**). The feldspars display variable degrees of alteration and dissolution and range from relatively fresh, unaltered grains to partly leached or near completely dissolved (skeletal) grains.

III. Glauconite

Glauconite is the third abundant mineral in this formation, which is displayed in the form of a kidney shape or sub rounded shape in some places. In most of the samples, especially in shallower ones, the glauconite occurs as a morphological glauconite, mainly in the form of sand-sized grains (pellets) indicating shallow marine environments. By increasing in depth, the number of glauconite grains decreased and they could be identified mostly as a secondary mineral infilling cracks and hollows or replacing pre-existing minerals.

In the study area, green to brown detrital grains are recorded which ranged from 2% to 11% by volume for W. Al khilala-2Well (**Fig. 14)** and ranged from trace quantities to 7% by volume for W. Al Khilala-5 Well (**Fig. 15**). Glauconite grains are well rounded to slightly elongated and are frequently altered and/or partly oxidized as in (**Fig. 18 & 19**).

IV. Lithic Fragments

The lithic fragments form a minor detrital component in most of the analyzed samples. The relative abundance ranges from traces to 6% in W. Al Khilala-2 Well (**Figs. 14 & 20**). In W. Al Khilala-5 it ranges from trace quantities to 5% by volume (**Fig. 15**).

V. Micas

Micas have been recorded in minor quantities ranging from trace quantities to 4% by volume in most of the analyzed samples for W. Al Khilala-2 Well (**Fig. 14**), while for W. Al Khilala-5 ranges from trace quantities to 8% by volume (**Fig. 15**). They are dominated by muscovite that occurs in the form of elongate, prismatic and needle-shaped grains (**Fig. 21**), which displays varying degrees of dissolution. The mica tends to accumulate in fine grain sediments (**Tucker, 1995**) in the ripple laminated and micro-deformed argillaceous sandstone samples.

VI. Heavy Minerals and Opaques

The heavy minerals are observed in most of the samples in amounts up to 2% of sample volume in W. Al Khilala-2 Well (**Fig. 14**), While in W. Al Khilala-5 Well ranges between trace quantities and 7% by volume in most of the analyzed samples (**Fig. 15**), which is represented in zircon and garnet, epidote, staurolite, tourmaline and zircon (**Fig. 22**), while the opaque minerals are represented with range from 1% to 5% by volume in all samples.

VII. Carbonaceous Debris

The carbonaceous debris detrital component occurs in some samples with relative abundances ranging up to 2% in W. Al Khilala-2 Well (**Fig. 14**), while in W. Al Khilala-5 Well ranges from trace quantities to 8% by volume (**Fig. 15**). The carbonaceous matter is represented by a needle to prismatic shaped plant debris, which is commonly aligned along argillaceous laminae (**Fig. 23**).

VIII. Phosphatic Fragments

The phosphatic fragments occur in some samples with relative abundances ranging up to 1.5% by volume (**Figs. 13 & 24**) for W. Al Khilala-2 Well, while for W. Al Khilala-5 well are recorded in trace quantities in few analyzed samples.

IX. Detrital Clays

The detrital clay is ranging from trace quantities to 38% by volume in some samples from the depths of 10125’, 10104’, and 10108’ for W. Al Khilala-2 well as displayed in (**Fig. 14**), while for W. Al Khilala-5 ranges from trace quantities to 91% by volume (**Fig. 15**). The detrital clays in the analyzed samples have been partially replaced by chlorite and/or illite (**Fig.25**).

4.4.2 Authigenic Components

The authigenic components are formed by the breakdown and alteration of feldspar, mica and rock fragments. These authigenic components are occupying the pore space leading to porosity reduction. In addition, they increase the microporosity of the total porosity causing permeability reduction, particularly in fine-grained samples.

In the study area, the authigenic components that are identified throughout the thin section and SEM analysis are calcite, quartz overgrowth, kaolinite, siderite, pyrite, chlorite and illite that described in more detail as follow:

I. Calcite / Dolomite

Calcite and dolomite are the major authigenic cements in the majority of analyzed samples. Dolomite and calcite cement occur as patchy pore filling and grain replacive phases. It ranges in W. Al Khilala-2 Well between 1.5% and 15% by volume (**Fig. 26)** and ranged in W. Al Khilala-5 Well between trace quantities and 3% (**Fig. 27**). They presented in the form of pore filling and rhombic crystals as displayed in (**Fig. 28**). The calcite occurs in most samples with relative abundances ranged between trace quantities and 20% by volume. They occurs mainly within rock fragments as a calcite cement (**Fig. 29**).

II. Quartz Overgrowths

The quartz overgrowth is presented from moderately to well-developed syntaxial quartz. It ranged from nil to 4% in W. Al Khilala-2 Well (**Fig. 26)**, while in W. Al Khilala-5 Well it ranged from 0.5% to 5% by volume (**Fig. 27)**. SEM observations revealed the presence of poorly to moderately developed euhedral, smooth-faced and pyramidal quartz overgrowths (**Fig. 30**).

III. Kaolinite

Kaolinite clay mineral occurs in the majority of analyzed samples with relative abundances ranging between nil and 7% in W. Al Khilala-2 Well (**Fig. 26**) and between trace quantities and 10% in W. Al Khilala-5 Well (**Fig. 27**). The SEM analyses indicate that kaolinite is the dominant clay mineral in the analyzed samples. It commonly occurs in the form of moderate to well crystallize, patchy and pore filling booklets. It shows vermiform texture and comprises partly corroded pseudo hexagonal basal plates (**Fig. 31**). The Kaolinite was probably generated at a late state in the diagenetic history of the sedimentary succession represented by the analyzed samples and is likely to represent the alteration product of feldspars and micas.

IV. Siderite

The siderite occurs only in deep six samples from 10054’ to 10125’. It constitutes from 1% to 26% of the samples in W. Al Khilala-2 Well (**Fig 26**) and from trace quantities to 5% in W. Al Khilala-5 Well (**Fig 27)**. Siderite occurs mainly as patchy, grain-replacive and microcrystals that have preferentially replaced clay matrix (**Fig. 32**).

V. Chlorite

Chlorite is represented in trace quantities in the majority of the analyzed thin sections. It commonly coats various detrital grains and replaces the detrital clay matrix. The SEM observations showed the presence of needle-like chlorite plates (**Fig. 33**). It locally replace detrital clay and glauconite pellets forming card-house texture.

VI. Illite

The illite mineral is presented in minor quantities which displayed by SEM analysis which shows the presence of hair-like illite (**Fig. 34**). It locally replaces detrital clay matrix and/or kaolinite plates.

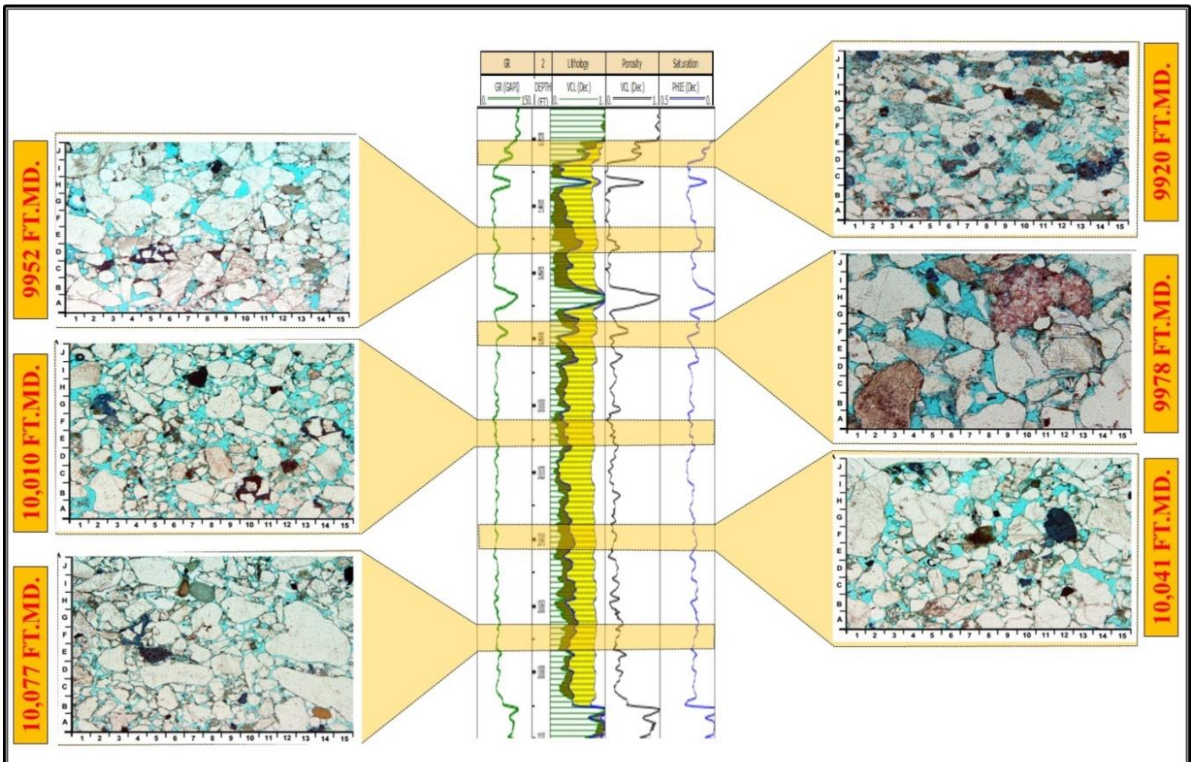

Fig. 12 : Thin section samples integrated with interperated logs for W. Al Khilala-2 Well.

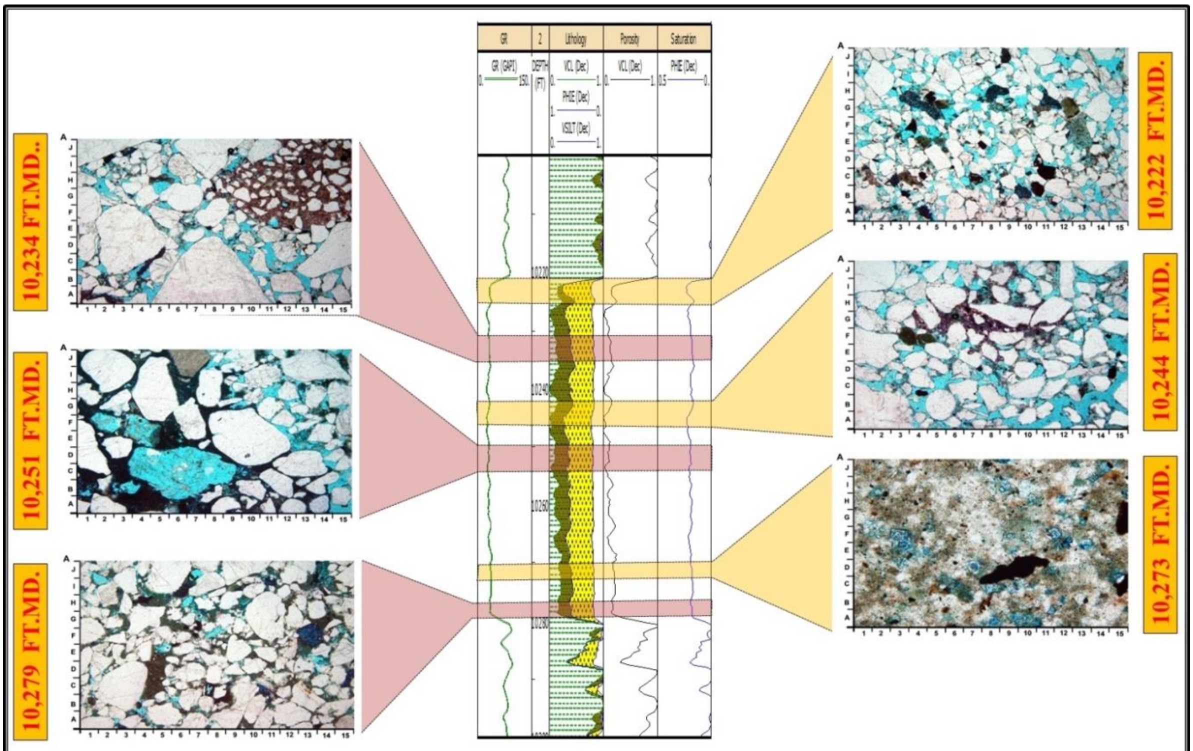

Fig. 13: Thin section samples integrated with interperated logs for W. Al Khilala-5 Well.

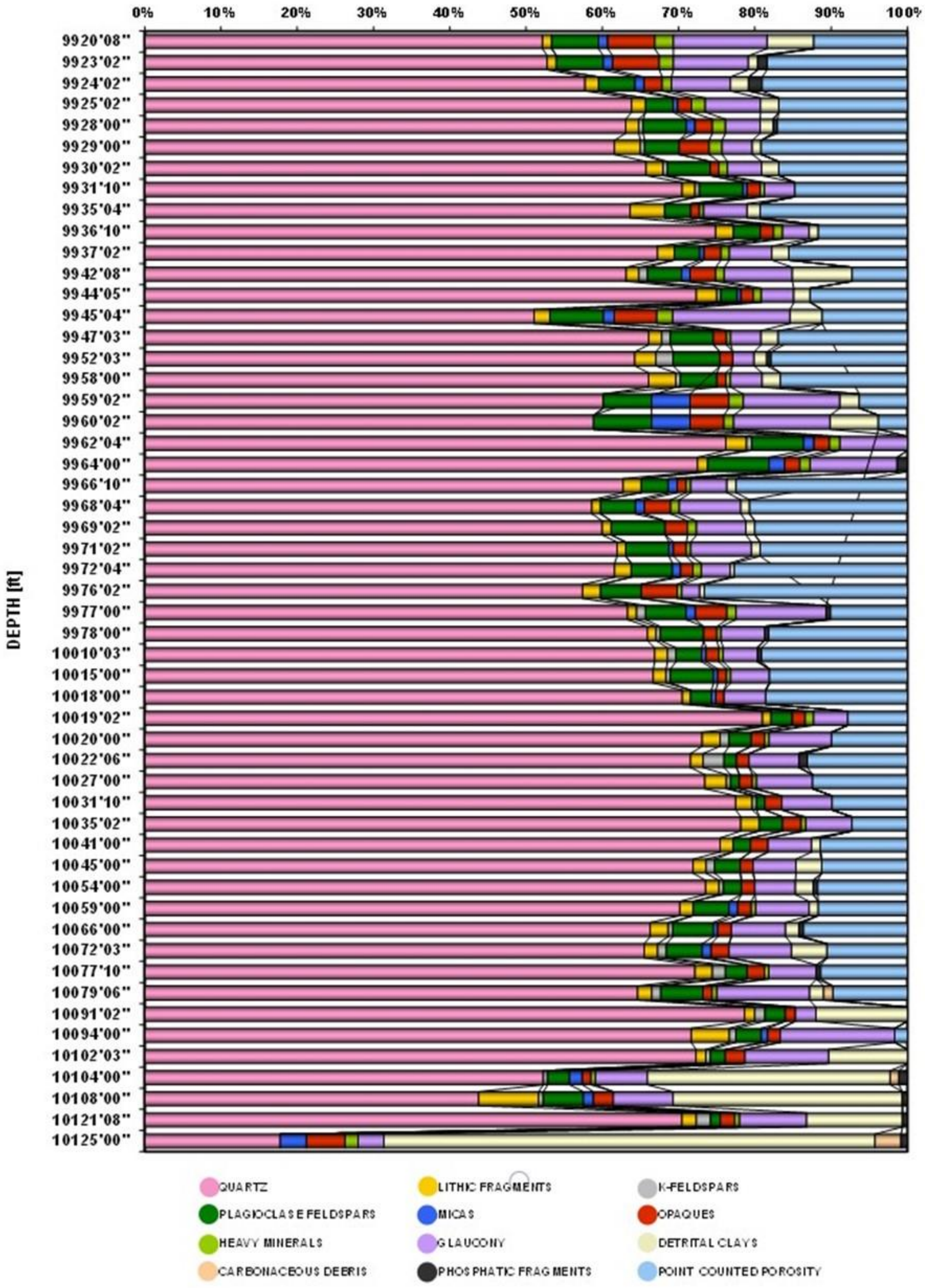

Fig.14 : Major Detrital Components and Point Counted porosuity value for Abu Madi Formation in W. Al Khilala-2 Well.

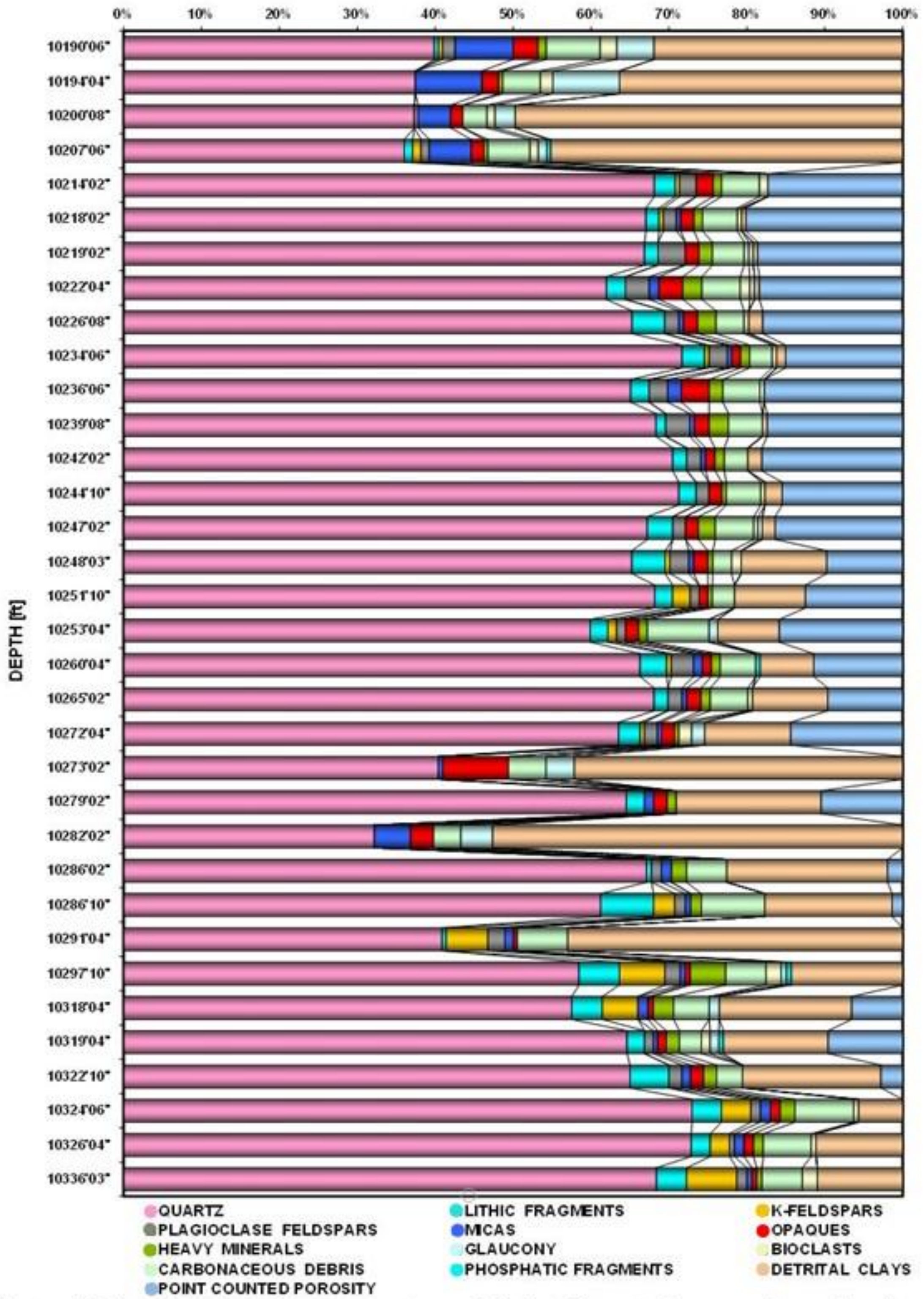

Fig.15: Major Detrital Components and Point Counted porosuity value for Abu Madi Formation in W. Al Khilala-5 Well.

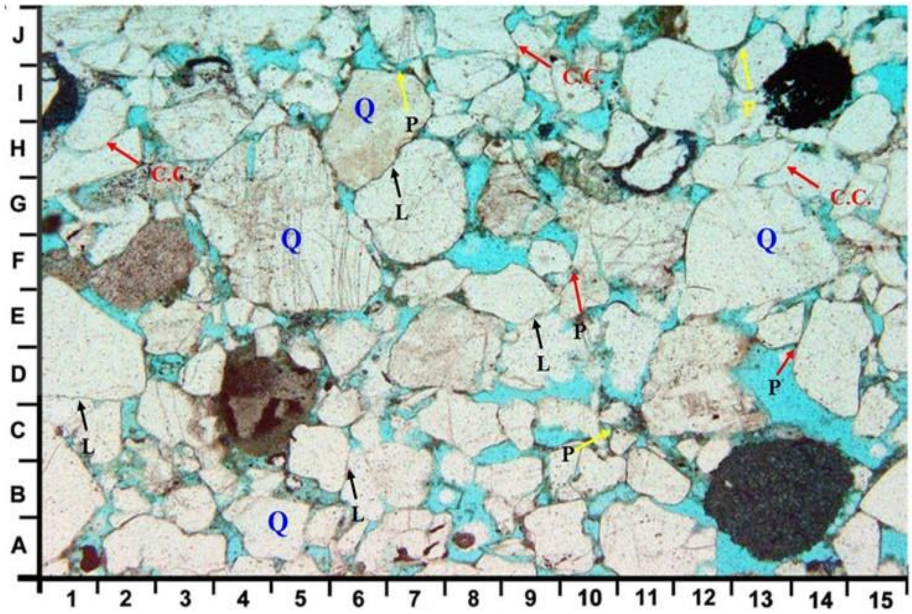

Description:-

Subfeldspathic arenite, fine to very coarse grained, poorly to moderately sorted, subangular to subrounded grains, poorly to moderately compacted displayed long (L), point (P), and concavo-convex (C.C) grain contacts.

Fig.16: Thin section photomicrography at the depth of 9931' displaying the reservoir grain roundness and compaction of quartz grains in Abu Madi Fm., at W. Al Khilala-2 Well.

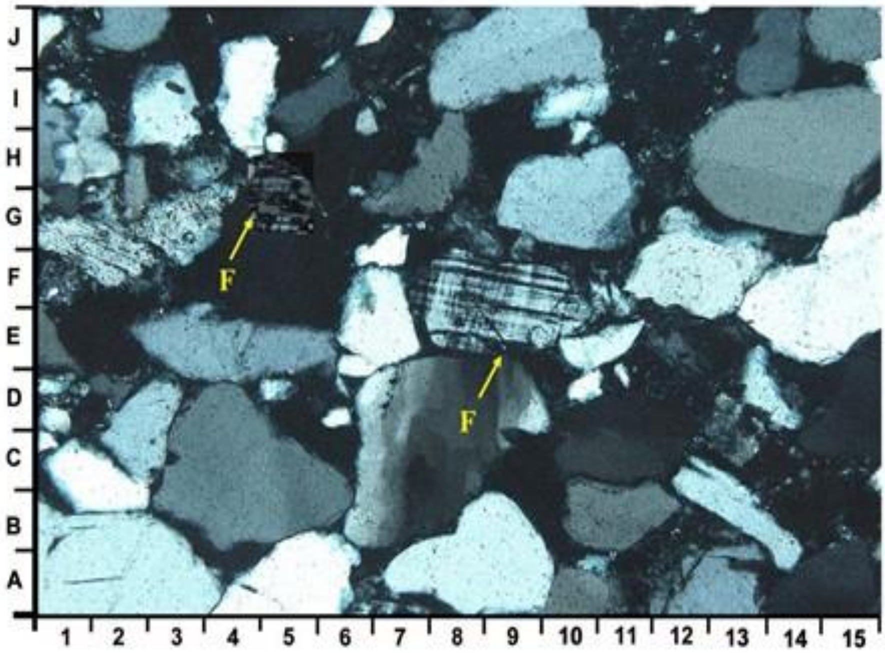

Fig. 17: Thin section photomicrography at depth 9928' displaying the feldspar grains (F) in Abu Madi Fm., W. Al Khilala-2 well.

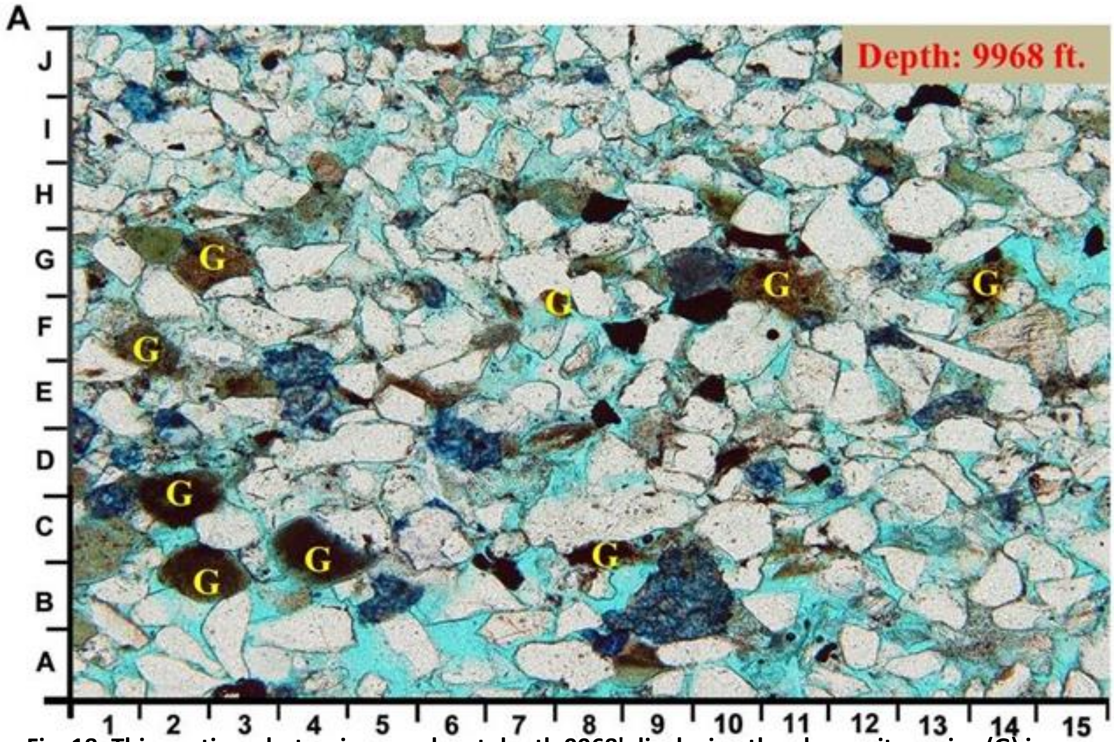

Fig. 18: Thin section photomicrography at depth 9968' displaying the glauconite grains (G) in Abu Madi Fm., W. Al Khilala-2 well.

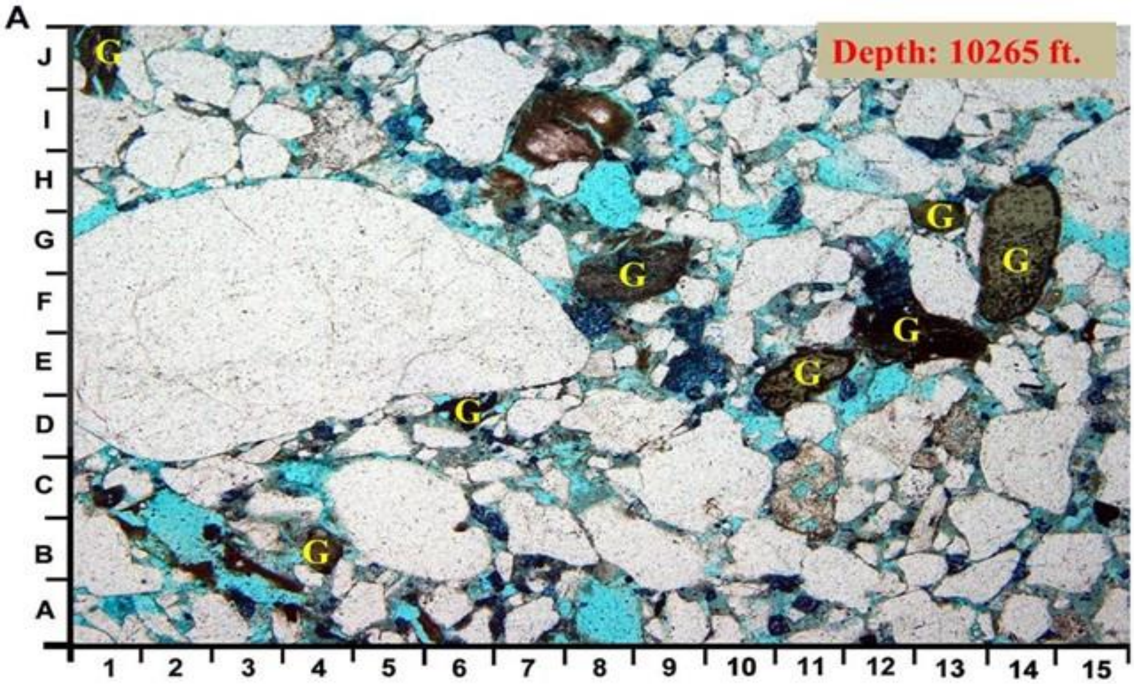

Fig. 19: Thin section photomicrography at depth 10265' displaying the glauconite grains (G) in Abu Madi Fm., W. Al Khilala-5 well.

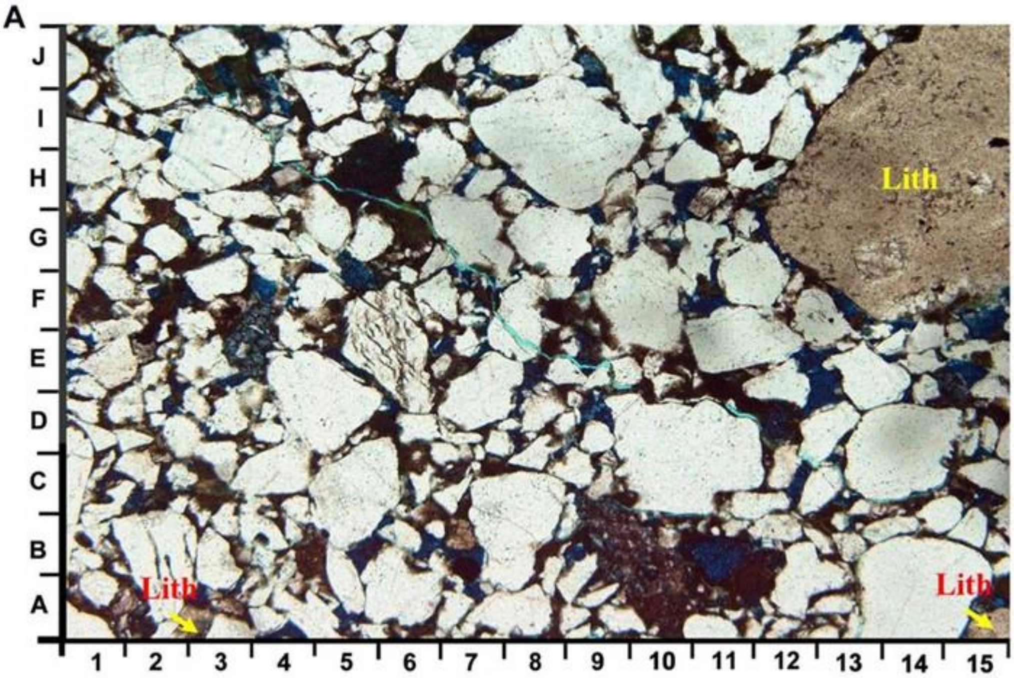

Fig. 20: Thin section photomicrography at depth 10108' displaying the lithic fragments (L) in Abu Madi Fm., W. Al Khilala-2 well.

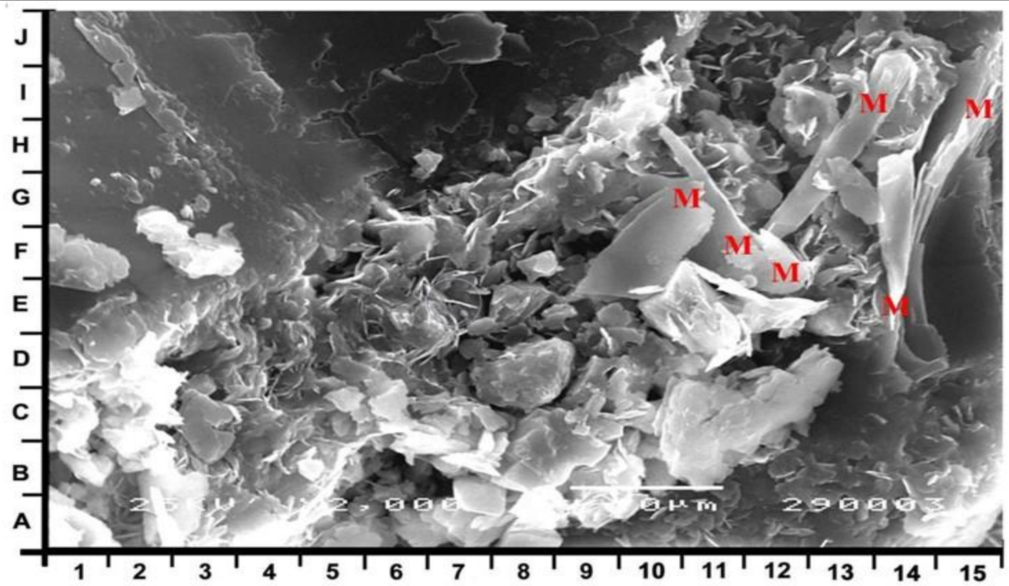

Fig. 21: SEM photography at depth 10072' displaying the Mica flakes (M) in Abu Madi Fm., W. Al Khilala-2 well.

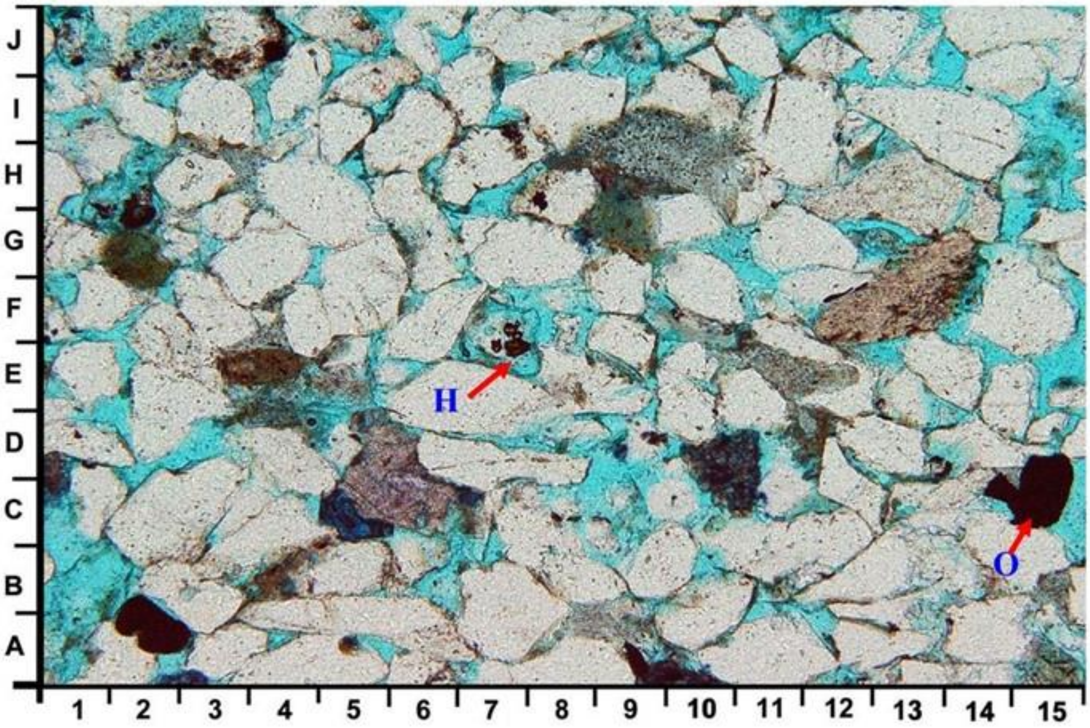

Fig. 22: Thin section photomicrography at depth 9924' displaying the heavy minerals (H) and opaque grains (O) in Abu Madi Fm., W. Al Khilala-2 well.

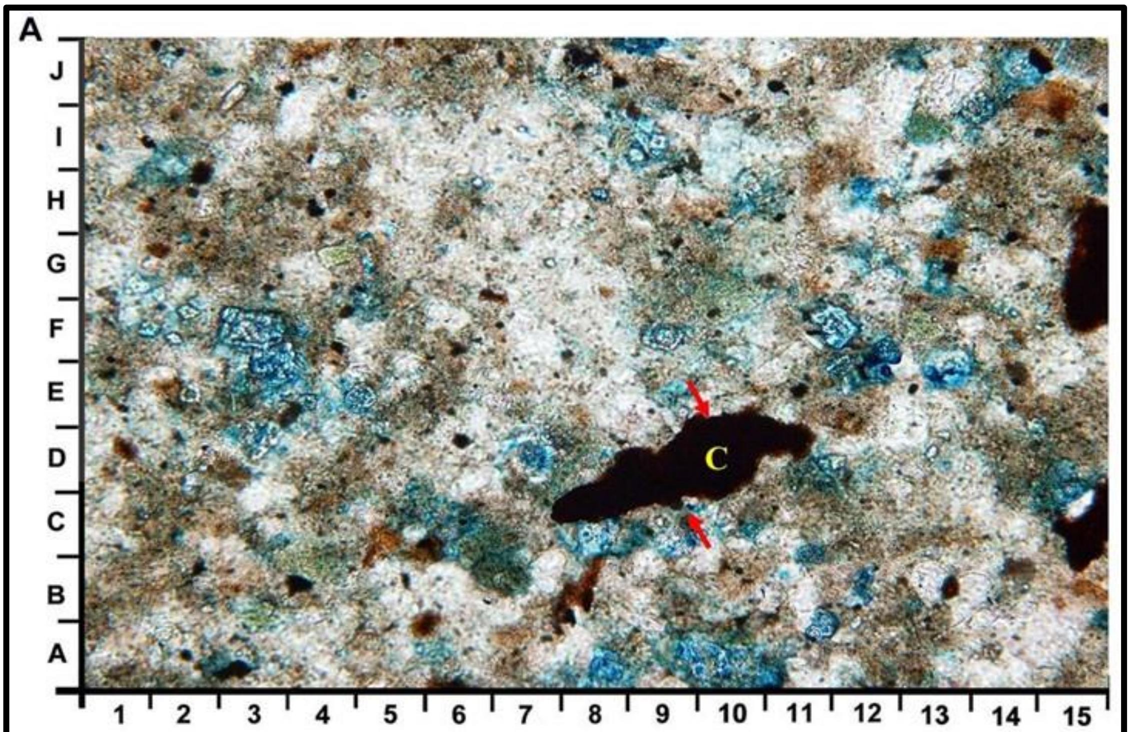

Fig. 23: Thin section photomicrography at depth 10273' displaying the carbonaceous debris (C) in Abu Madi Fm., W. Al Khilala-5 well.

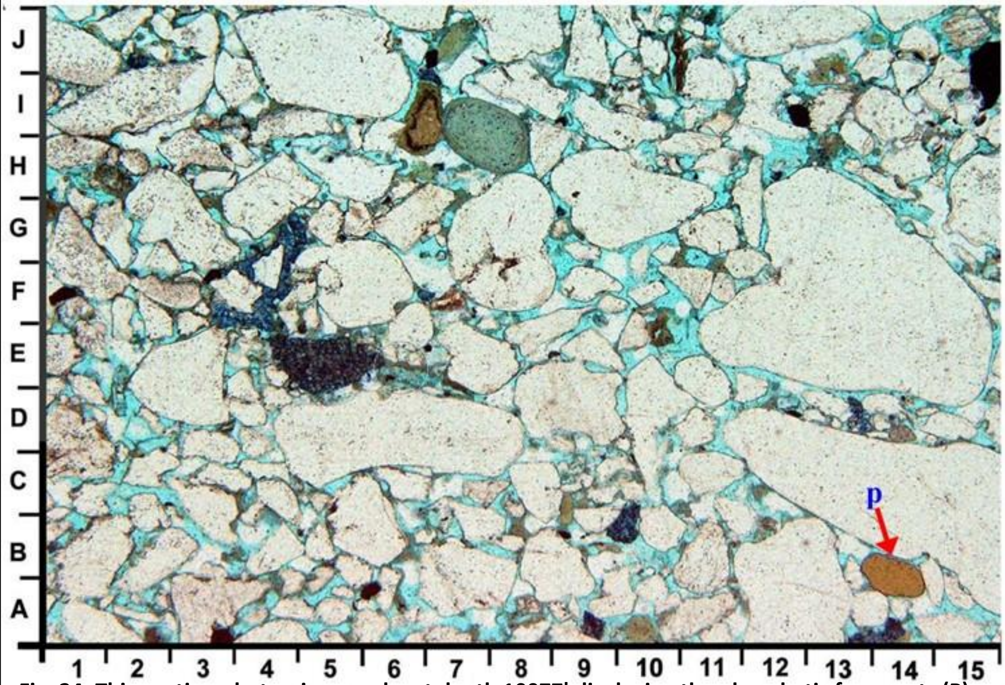

Fig. 24: Thin section photomicrography at depth 10077' displaying the phosphatic fragments (P) in Abu Madi Fm., W. Al Khilala-2 well.

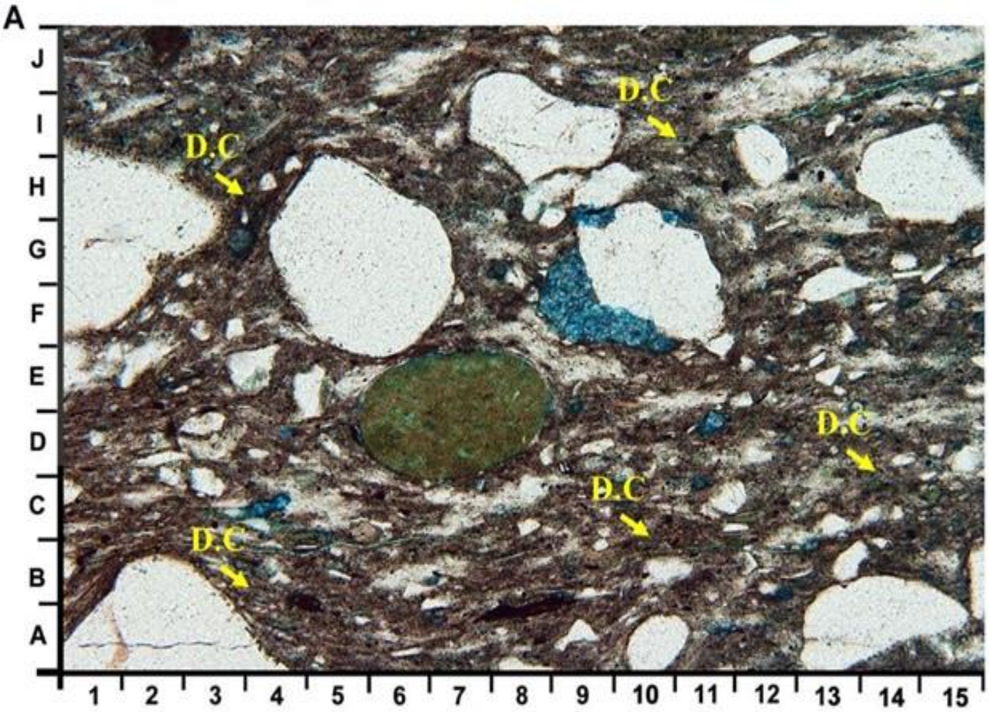

Fig. 25: Thin section photomicrography at depth 10104' displaying the detrital clays grains (D.C) in Abu Madi Fm., W. Al Khilala-2 well.

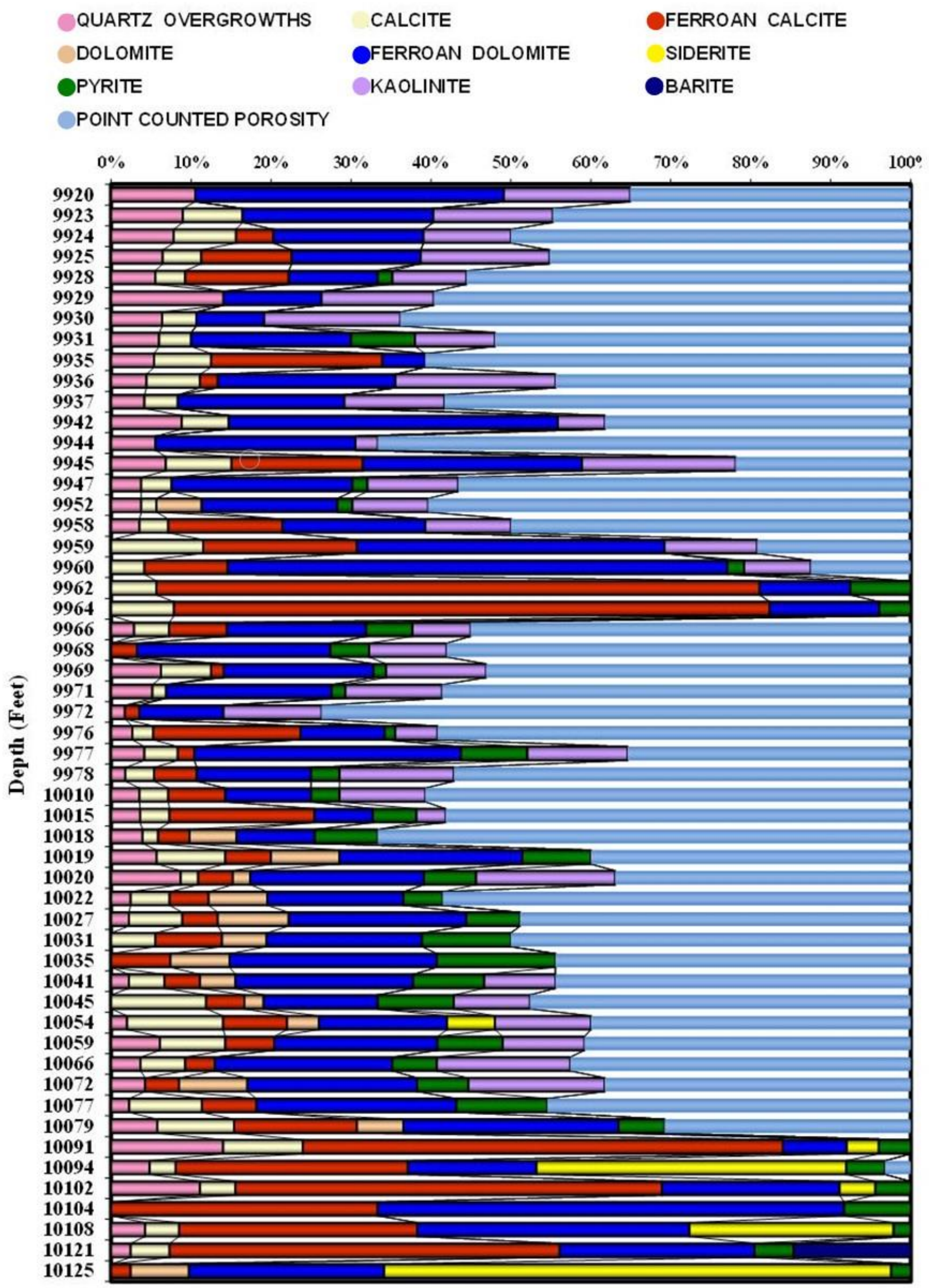

Fig. 26 : Major authigenic components (in percent per volume) For Abu Madi Formation in W. Al Khilala-2 Well.

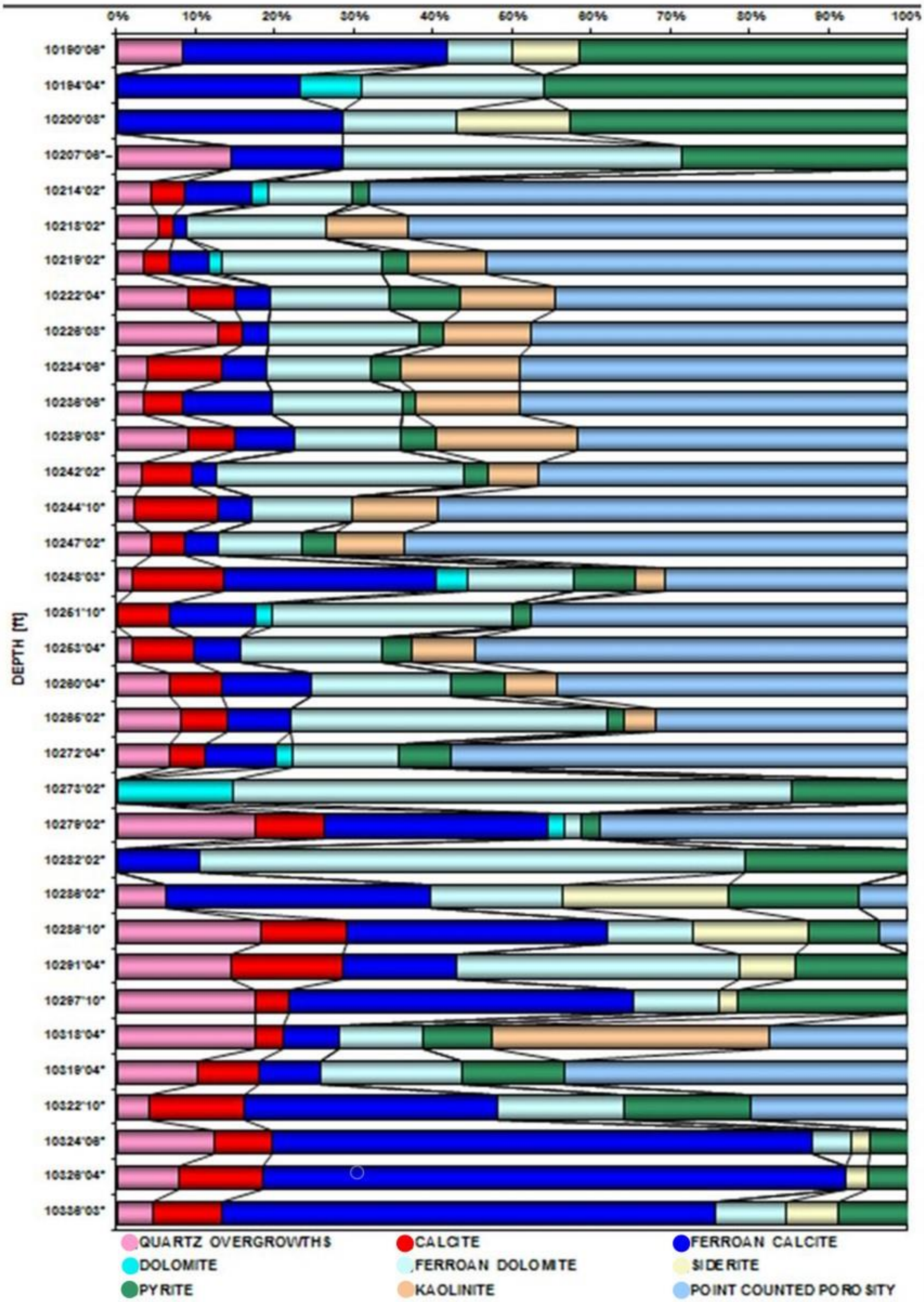

Fig.27 : Major authigenic components (in percent per volume) For Abu Madi Formation in W. Al Khilala-5 Well.

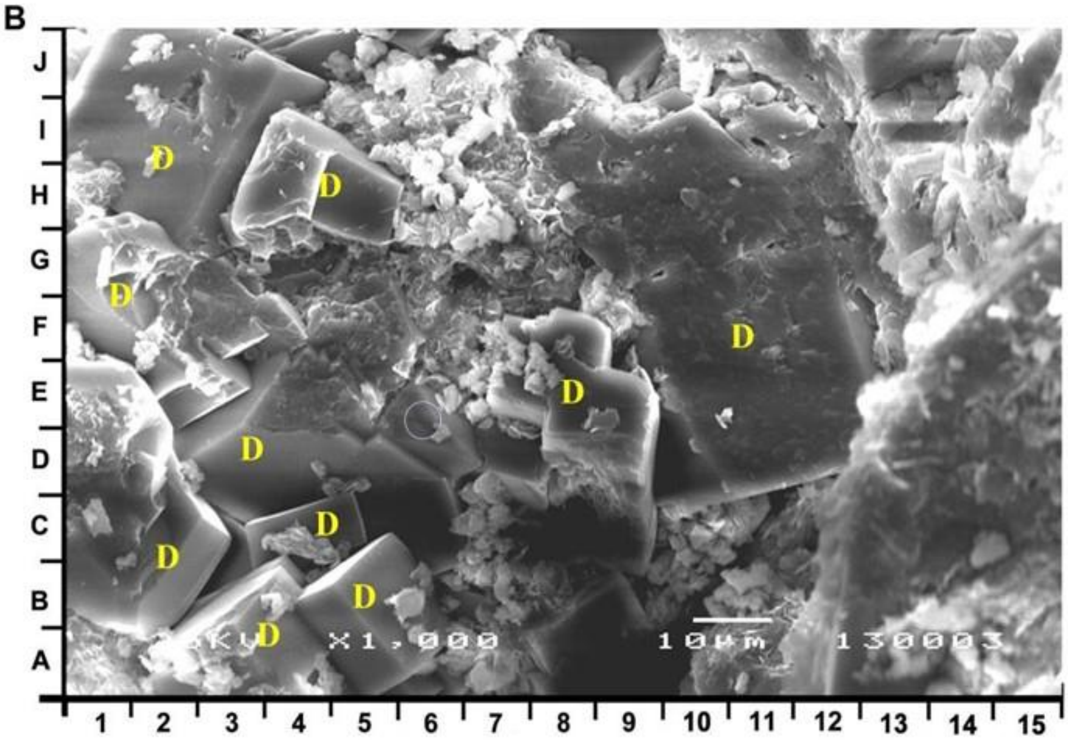

Fig. 28: SEM photomicrography at depth 9959' displaying the dolomite authigenic fragments (D) in Abu Madi Fm., W. Al Khilala-2 well.

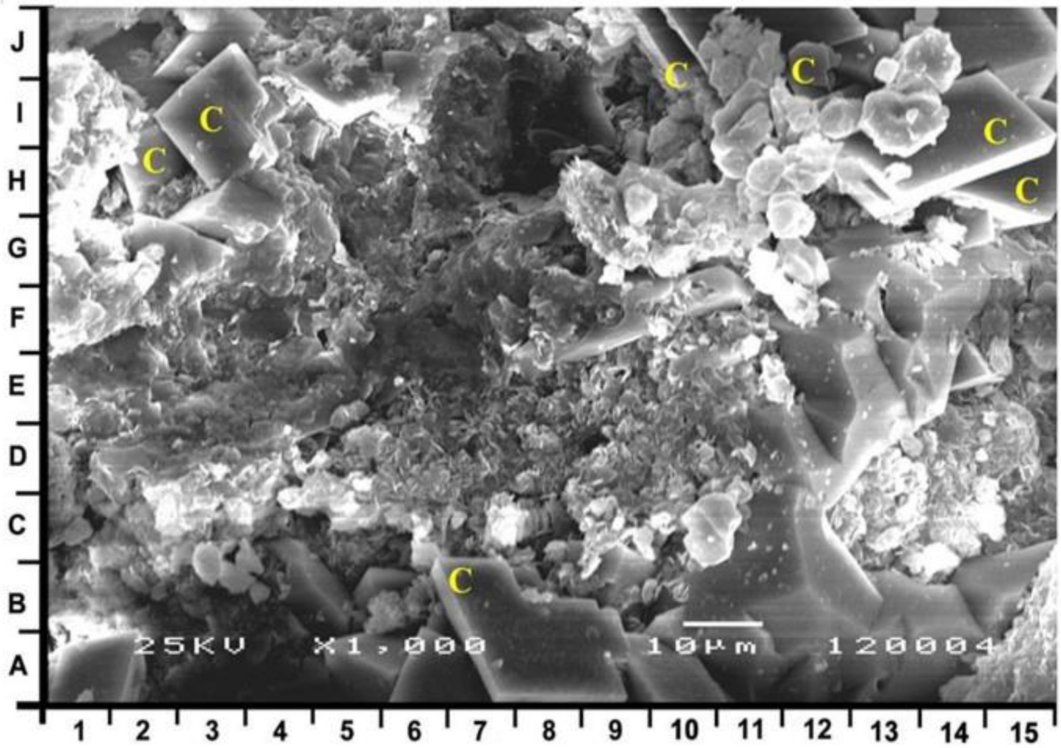

Fig. 29: SEM photomicrography at depth 9958' displaying the calcite authigenic fragments (C) in Abu Madi Fm., W. Al Khilala-2 well.

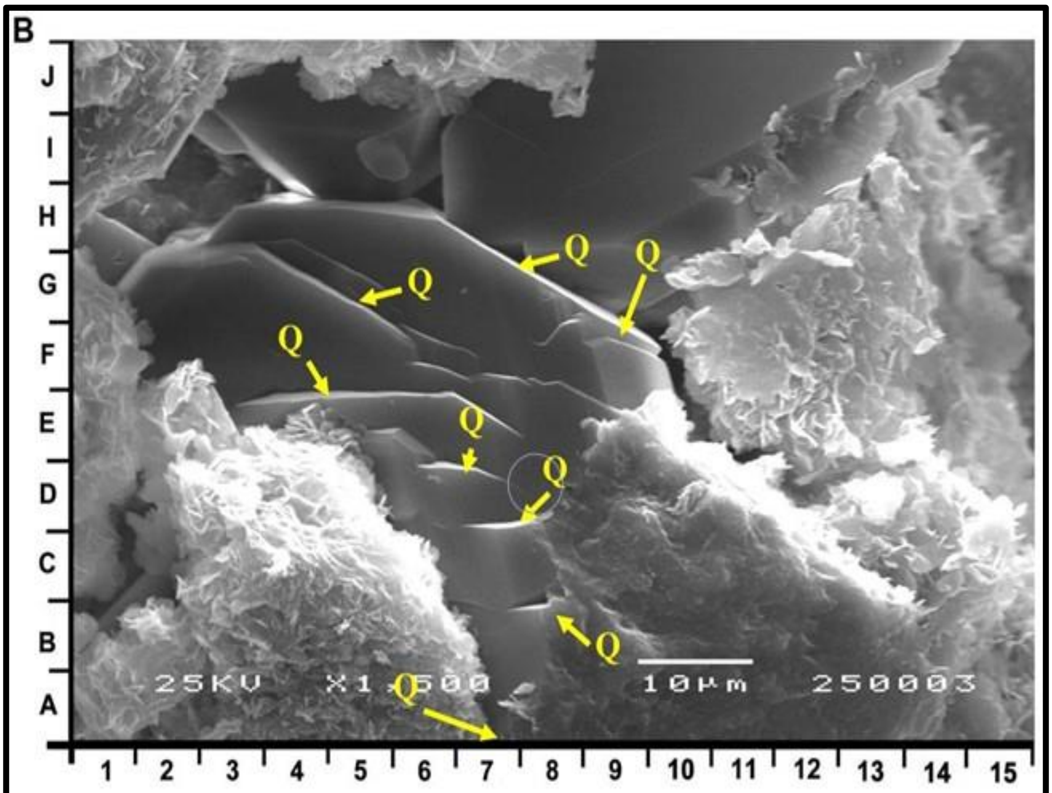

Fig. 30: SEM photomicrography at depth 10031' displaying the quartz overgrowth (Q) in Abu Madi Fm., W. Al Khilala-2 well.

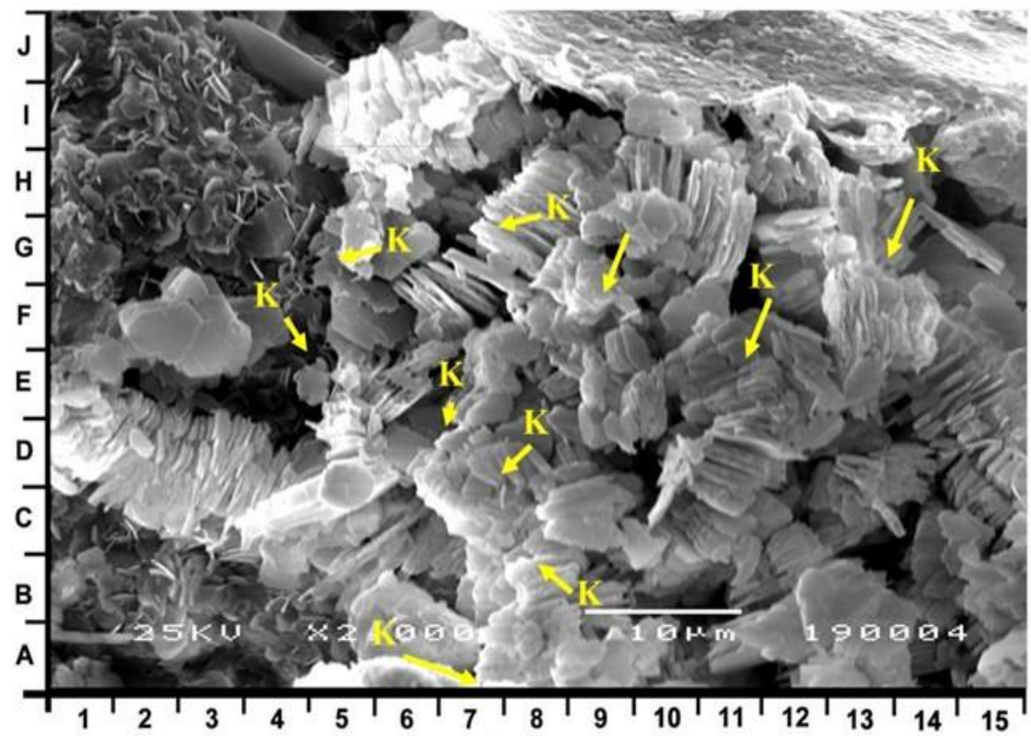

Fig. 31: SEM photomicrography at depth 9978' displaying the kaolinite (K) in Abu Madi Fm., W. Al Khilala-2 well.

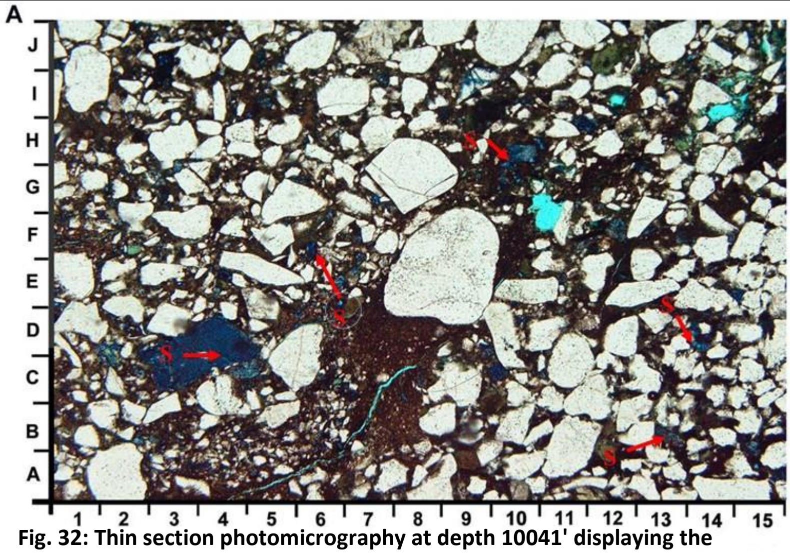

Fig. 32: Thin section photomicrography at depth 10041' displaying the sedrite fragments (S) in Abu Madi Fm., W. Al Khilala-2 well.

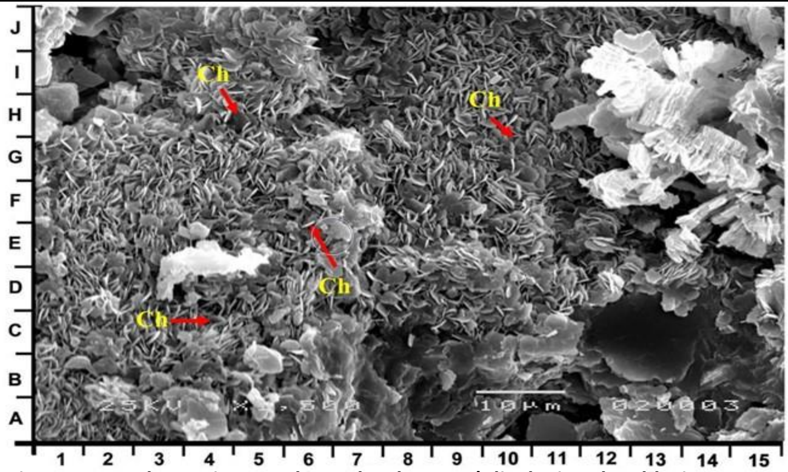

Fig. 33: SEM photomicrography at depth 10010' displaying the chlorite fragments (Ch) in Abu Madi Fm., W. Al Khilala-2 well.

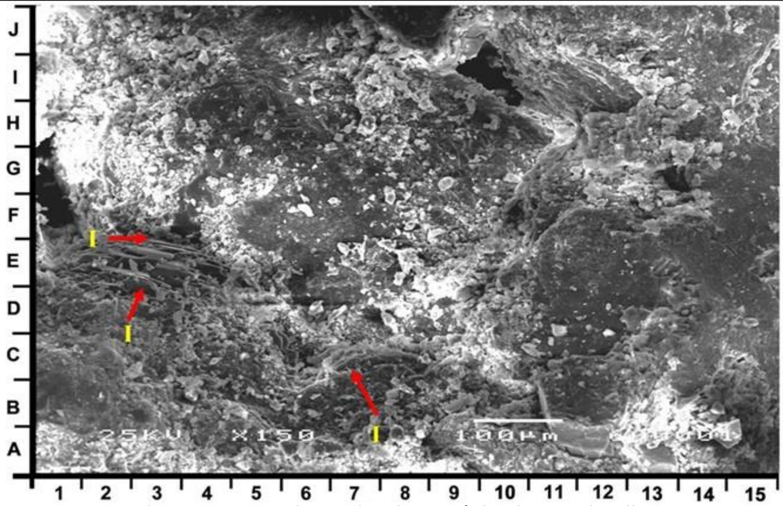

Fig. 34: SEM photomicrography at depth 9935' displaying the illite fragments (I) in Abu Madi Fm., W. Al Khilala-2 well.

5. Conclusions

This study holds significant importance for the oil and gas industry, particularly for operators involved in the exploration and development of reservoirs in the W. AL Khilala Field. It elucidates the reservoir characteristics and behavior. It aims to contribute valuable insights that can inform decision-making processes related to reservoir management, field development planning, and production optimization. Additionally, the findings of this study serve as a basis for future research endeavors aimed at further enhancing our understanding of similar hydrocarbon-bearing formations. Ultimately, the outcomes of this study are expected to facilitate more efficient and sustainable hydrocarbon extraction practices, thereby contributing to the long-term viability and profitability of the W. AL Khilala Field.

References

Abd El Aal, A., Price, R. J, Vaitl, J. D. and Shrallow, J. A. (1994): Tectonic evolution of the Nile Delta, its impact on sedimentation and hydrocarbon potential, EGPC., Proc. of the 12th Pet. Conf., Cairo, Vol. 12, No. I, pp 19-34.

Argyriadis, I., Graciansky, P. C., Marcoux, J. and Ricou, L. E. (1980): The opening of the Mesozoic Tethys between Eurasia and Arabia-Africa, Mem. du Bureaude de Recherche Geologiques et Minieres, Vol. 115, pp 199-214.

Bateman, R. (1985): Open hole log analysis and formation evaluation, Boston International Human Resources Development Corporation, 647 p.

Egyptian General Petroleum Corporation, (1994): Nile Delta and north Sinai Fields, discoveries and hydrocarbon potential (a comprehensive overview). The Egyptian Petroleum Corporation, Cairo, Egypt, 387 p.

El Heiny, I. (1982): Neogene stratigraphy of Egypt, Newslett. Stratig., Vol. 11, No. 2, pp 41-54.

El Heiny, I. and Enani, N. (1996): Regional stratigraphic interpretation pattern of Neogene sediments, northern Nile Delta, Egypt, 13th EGPC., Expl. Pet. Conf., Cairo, Vol. 1, pp 270-290.

El Heiny, I. and Morsi, S. (1992): Stratigraphic correlation of Neogene sediments in the eastern Nile Delta and Gulf of Suez, Egypt, 11th EGPC., Expl. and Prod. Conf., Cairo, Vol. 1, pp 1- 28.

Elbosraty, M. (2005): Sequence stratigraphy of the Nile Delta with emphasis on the basin analysis, unpublished Ph. D. thesis, Ain Shams Univ., Egypt, 282 p.

Elgamal, M. (2001): One of a kind the birth and abortion of the mid Nile Delta Oligocene rift deserving attention by petroleum explorationists, In: Deltas modern and ancient (Zaghloul, Z. and Elgamal, M. 2001 edits.), pp 229-237.

Elgamal, M. (2002): The prospectively of Qantara concession with emphasis on the Lower Miocene Qantara Formation. Qantara Pet. Co. (Int. Rep.).

Elgamal, M. and Elbosraty, M. (2008): The driving forces behind the tectonics and evolution of the southeastern Mediterranean, with the hydrocarbon systems relationship and future discoveries, MOC., Alex., Egypt, 69 p.

Elhamy A. T. and Salah S. A. (2016): Structural Effect on Hydrocarbon Trapping, North Western Nile Delta, Egypt, Inter. Jour. Geosci., Vol. 7, pp 353-366.

El-Shafei, I. (2004): Geophysical studies and GIS application on Abu Madi gas field, Nile Delta, Egypt. M.Sc. Thesis, Geology Department, Faculty of Science, Helwan University, Egypt, 162 P.

Harwood, C., Hodgson, N. and Ayyad, M. (1998): The Application of Sequence Stratigraphy in the Exploration for Plio-Pleistocene Hydrocarbons in the Nile Delta, EGPC., Proc. of the 14th Expl. and Prod. Conf., Cairo, Egypt.

Ismail A., Radwan A., Leila M. and Eysa, E.A. (2024): Integrating 3D subsurface imaging, seismic attributes, and wireline logging analyses: Implications for a high resolution detection of deep-rooted gas escape features, eastern offshore Nile Delta, Egypt, Journal of African Earth Sciences 213 (2024), 13 p.

Khaled K. A., Attia, G. M., Metwalli, F. I. and Fagelnour, M. S. (2014): Subsurface Geology and Petroleum System in the Eastern Offshore Area, Nile Delta, Egypt, Jour. of Applied Sci. Research, Vol. 10, No. 4, pp 254-270.

Levorson, A. I. (1967): Geology of Petroleum. W. H. Freeman and San Francisco, 350 p.

Mahsoub, M. A. (2006): Facies and stratigraphy of the sedimentary sequence of Abu Qir West Field, Nile Delta-Egypt, unpublished M. Sc. thesis, Ain Shams Univ., Egypt, 220 p.

Mansoura Pet. Co. (2005): Final Geological Report of W. Al Khilala-1 Well. (Interal report)

Mansoura Pet. Co. (2008d): Final Geological Report of W. Al Khilala-5 Well.

Nashaat, M. (1998): Abnormally high fluid pressure and seal impacts on hydrocarbon accumulations in the Nile Delta and North Sinai Basins, In: Abnormal Pressures in Hydrocarbon Environments, (Law, B.E., Ulmishek, G.F. and Slavin, V.I., 1998 edits), AAPG Bull., Vol. 70, pp 161-180.

Nashaat, M. (2000): The petroleum system from source rock to trap in the Nile delta and North Sinai offshore basins, Egypt, implications of overpressure on hydrocarbon accumulation, MOC., Alex., Egypt, 10 p.

Rizzini, A., vezzani, F., Coceccetta, V. and Milad, G. (1978): Stratigraphy and sedimentation of Neogene-Quaternary section in the Nile Delta area, Marine Geol., Vol. 27, pp 327-348.

Said, R. (1990): The geology of Egypt, Balkema, A. A., Rotterdam, Netherlands 734 p.

Schlumberger (1984): Well Evaluation Conference, Egypt (WEC), 1st edit., Cairo, Egypt, 245 p.

Tucker, M.E. (1995): Sedimentary Petrology, an introduction to the origin of sedimentary rocks. 2nd edits., Blackwell Sci. Publ., Oxford, 260 p.